The present work was submitted to the Institute for Biology II, Unit of Zoology and Human Biology, RWTH, University of Aachen

Pluripotent Embryonic Stem Cells Development and Differentiation under Altered Gravity Conditions

Master thesis submitted in fulfillment of the requirements for the degree Master of Science in Biology

Faculty of Mathematics, Computer Science and Natural Sciences, Department of Biology, RWTH University of Aachen

presented by

Wegener, Lucia

from Hannover, Germany

Name of 1st examiner: PD Dr. Ruth Hemmersbach, German Aerospace Center (DLR), Cologne

Name of 2nd examiner: Prof. Dr. Johannes Bohrmann, RWTH Aachen

Aachen, January 2016

Affirmation for the Master's Thesis

I herewith declare, that I have written this thesis independently and by myself. I have used no other sources than those listed. I have indicated all places from where the exact words or analogous text were taken as sources. I assure that this thesis has not been submitted for examination elsewhere.

Aachen, _____ _____

Table of Contents

Table of Contents IV

1 Introduction 1

1.1 Effects of Microgravity and Hypergravity on the Development of Life 1

1.2 Microgravity Simulators and Hypergravity Facilities 3

1.3 Embryonic Stem Cells (ESCs) 4

1.4 Cardiomyogenesis 6

1.5 Cell Cycle 7

1.6 The Cytoskeleton in Altered Gravity 9

1.7 Aim of this Study 10

2 Materials and Methods 12

2.1 Materials 12

2.1.1 Consumables 12

2.1.2 Reagents 13

2.1.3 Kits 14

2.1.4 Nucleotide Sequences 15

2.1.5 Cell Culture Media 15

2.2. Methods 16

2.2.1 Cell Culture 16

2.2.2 Simulated Microgravity Experiments 18

2.2.3 Embryoid Body Collection and Further Processing 20

2.2.4 Hypergravity Experiments 21

2.2.5 Embryoid Body Collection and Further Processing 22

2.2.6 Cytoskeleton Staining (Phalloidin/DAPI) 23

2.2.7 Flow Cytometry 24

2.2.8 RNA Isolation and cDNA Synthesis 26

2.2.9 Reverse Transcriptase Quantitative Real-Time Polymerase Chain Reaction (qRT-PCR) 28

Table of Contents

2.2.10 Embryoid Body Morphology 29
2.2.11 Statistical Analysis 30
3 Results 31
3.1 Simulated Microgravity Experiments 31
3.1.1 Macroscopic and Microscopic Observations: Cytoskeleton 31
3.1.2 Effect of Simulated Microgravity on the Cell Cycle 33
3.2 Hypergravity Experiments 36
3.2.1 Embryoid Body Morphology and “Beating” Activity 36
3.2.1.1 Changes in the Morphology of Embryoid Bodies 38
3.2.1.2 Embryoid Body “Beating” Activity 41
3.2.2 Microscopic Observations: Cytoskeleton 42
3.2.3 Effect of Hypergravity on the Cell Cycle 44
3.2.4. Comparison of Cell Cycle Distribution of the two 1 g Control Groups 46
3.2.5 Effect of Hypergravity on the Gene Expression 47
4 Discussion 49
4.1 Simulated Microgravity Experiments 49
4.1.2 Simulated Microgravity affects the Actin Cytoskeleton 49
4.1.2 Effects of Simulated Microgravity on the Cell Cycle 50
4.2 Hypergravity Experiments 53
4.2.1 Hypergravity affects the Actin Cytoskeleton and Embryoid Body Morphology 53
4.2.2 Effects of Hypergravity and Vibrations as Possible Side Effect on the Cell Cycle 54
4.2.3 Altered Gene Expression and Cardiomyogenesis in Hypergravity 55
4.3 Conclusion and Outlook 56
5 Summary 58
Acknowledgment 60
References 61
Appendix 68

1 Introduction

Over the last billions of years, gravity has been an ever-present environmental factor during the creation of life and in evolution, affecting the phylogenetic development of all living organisms (Anken and Rahmann, 2002). Gravity is the oldest known stimulus, which compelled the ancestors of all extant living beings to develop basic achievements to counter the gravitational force (e.g. elements of statics like any kind of skeleton). Already early forms of life possibly used gravity as an appropriate cue for orientation and control, since it is continuously present and has a fixed direction (Anken and Rahmann, 2002). The influence of gravity is not well understood, however, except that there is a clearly visible biological response to gravity in the structure and functioning of living organisms (e.g. gravity sensors in plants, in animals or even in humans) (Clément, 2005). By altering the influence of the gravity vector, it is possible to investigate its impact on cell activity and functional parameters of interest. In the present study, the influence of altered gravity (i.e. microgravity and hypergravity) at the cellular level was investigated.

1.1 Effects of Microgravity and Hypergravity on the Development of Life

There are many studies, which have been performed during spaceflight and in ground-based facilities (GBF, microgravity simulators) to investigate the influence of microgravity (µ *g*) on the development of cells, plants, animals and humans, which suggested that many cell types are sensitive to the microgravity environment (e.g. Wakayma et al., 2009; Buravkova et al., 2008; Wang et al., 2011; Wakayma et al., 2009; Crawford-Young, 2006; Serova et al., 1982). Moreover, experiments during space missions such as Cosmos 1129 and STS-80 have demonstrated that microgravity affected the reproduction and the early embryogenesis of rodents (rats and mice) (Crawford-Young, 2006; Wakayama et al., 2009; Serova et al., 1982; Kojima et al., 2000). For example, rats were allowed to mate in space, but the females failed to become pregnant, although fertilization had occurred (Serova et al.; 1982, Crawford-Young, 2006), and

mouse 2-cell embryos did not show any sign of development during the exposure to microgravity (Crawford-Young, 2006).

Furthermore, experiments were performed with amphibians such as *Xenopus laevis* or *Pleurodeles waltl*. By using ground-based facilities (GBF, see chapter 1.2) such as clinostat to simulate the influence of microgravity on the development of early staged embryos of *Xenopus*, it was shown that there were changes at all stages of development in comparison to the development under normal gravity conditions (1 *g*) (Crawford-Young, 2006; Neff et al., 1993). These changes during development in simulated microgravity resulted in a different morphology of the hatching embryos: they had a larger head, larger eyes and an arched back (Neff et al., 1993; Crawford-Young, 2006). Also salamanders (*Pleurodeles waltl)* revealed to have problems during development in real microgravity. They showed abnormalities in the neural tube closure in the head or cephalic region (Crawford-Young, 2006).

Studies in order to analyze the underlying mechanism, microgravity as well as hypergravity (h *g*) experiments focus on gravity induced-alterations at the cellular level and thus the early development of embryonic stem cells and embryogenesis (Wang et al.; 2011, Shinde et al., 2015; Kawahara et al., 2009). Wang et al. (2011) analyzed various effects of simulated microgravity on e.g. cell cycle distribution, cell differentiation, cell adhesion, apoptosis, genomic integrity and DNA damage repair in murine embryonic stem cells (mESCs). These results indicated that mESCs are sensitive to simulated microgravity in adapting with respect to cellular events (Wang et al., 2011; Buravkova et al., 2008). There were also some studies performed under h *g* conditions, which focused on genes that are involved in forming the cytoskeleton as well as those encoding growth factors (Ma et al., 2013). The exposure of cell lines *in vitro* to parabolic flights showed that hypergravity and vibrations, both occurring during parabolic flights, affected the behavior and development of cells and their gene expression (Ma et al., 2013).

Current research focuses on the development and embryogenesis in weightlessness in order to understand the development of biosystems in the context of altered gravity. Regarding this issue, hypergravity provides a further condition to study the impact of gravity on the development.

These kinds of studies are still at the beginning and many aspects can be investigated (e.g. cell cycle, differentiation, morphological changes, gene expression and cytoskeleton).

1.2 Microgravity Simulators and Hypergravity Facilities

A number of ground-based facilities based on different physical principles exist, aiming at a simulation of microgravity such as the 2D and 3D clinostat, the random positioning machine, the rotating wall vessel and diamagnetic levitation (Brungs et al., 2016; Herranz et al., 2013). These approaches are used to investigate the effect of simulated microgravity on e.g. the development of embryos and embryonic stem cells as well as on cell structure, gene expression and differentiation of cardiomyocytes (Crawford-Young; 2006; Hemmersbach et al., 2006; Herranz et al., 2013; Wang et al., 2011; Shinde et al., 2015). Furthermore, centrifuges are used for the exposure of biosystems to hypergravity conditions such as the Multi Sample Incubator Centrifuge (MuSIC) and the Short Arm Human Centrifuge (SAHC), which are both located at the German Aerospace Center at Cologne, Germany (Frett et al., 2015).

The 2D clinostat technique allows the rotation of samples (typically in liquid media) around an axis perpendicular to the direction of the gravity vector at a certain speed (usually at 60 rpm). Under these conditions the gravity vector is constantly turned, reaching according to the working hypothesis residual accelerations which are no longer perceived by the exposed systems (figure 1) (Herranz et al., 2013; Brungs et al. 2013). Dedicated centrifuges are used to create a hypergravity environment (up to 40 *g*) for cell cultures, plants, aquatic systems up to humans (Frett et al., 2015).

The use of ground-based facilities to simulate microgravity and to create hypergravity is a convenient way to study the effects of altered gravity conditions *in vitro* on the early development and the embryogenesis. Furthermore, they are essential for preparing experiments under real microgravity (e.g. spaceflights) conditions.

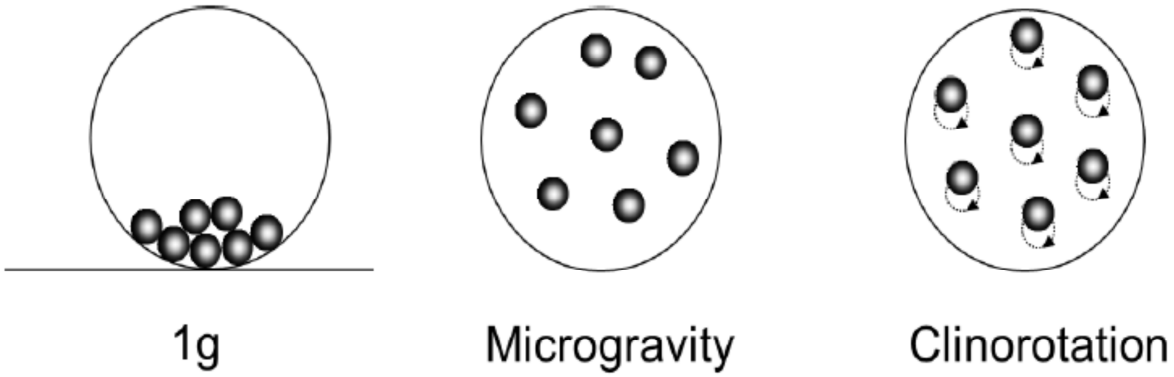

Figure 1: The principle of clinorotation: cells in liquid media will sediment under normal gravity conditions (1 *g*) (left). Cells under real microgravity conditions will be randomly distributed and weightless (center). By the exposure on a 2D clinostat, cells will be rotated along one axis perpendicular to the direction of the gravity vector; microgravity is simulated due to the neutralization of sedimentation (right) (from Häder et al., 2005)

1.3 Embryonic Stem Cells (ESCs)

Stem cells are pluripotent cells, which are commonly defined as undifferentiated cells that can proliferate. They have the capability of both self-renewal and differentiation to a number of various types of specialized cells (Rippon and Bishop, 2004). ESCs were first isolated in 1981 by using culture techniques which are based on the experience with the culture of ordinary stem cells. Embryonic stem cells are pluripotent stem cells, derived from the inner cell mass of a blastocyst, an early stage preimplantation embryo (figure 2) (Evans and Kaufman, 1981; Thompson et al., 1998; Itskovitz-Eldor et al., 2000). Pluripotency is the competence of cells to differentiate into any of the three germ layers (ectoderm, endoderm and mesoderm) and is one of the major properties of ESCs. These cells are distinguished by their ability to stay in an undifferentiated state *in vitro* by special culture conditions. While embryonic stem cells can generate all cell types in the body, adult stem cells are multipotent and can produce only a limited number of cell types.

Embryonic stem cells have a normal karyotype, maintaining a high telomerase activity and exhibiting a remarkable long-term proliferative potential (Bishop et al., 2002; Rippon and Bishop, 2004). Cells of the inner cell mass lastly continue to generate the embryo proper and therefore have the capacity to form all the tissues in the body. The three distinct layers are formed after a blastocyst´s inner cell mass undergoes a process of specific organization (gastrulation), which occurs after the blastocyst phase in embryonic development. Gastrulation involves many issues including distinct differentiation patterns, cell shape and cell adhesion (Rowland, 2009).

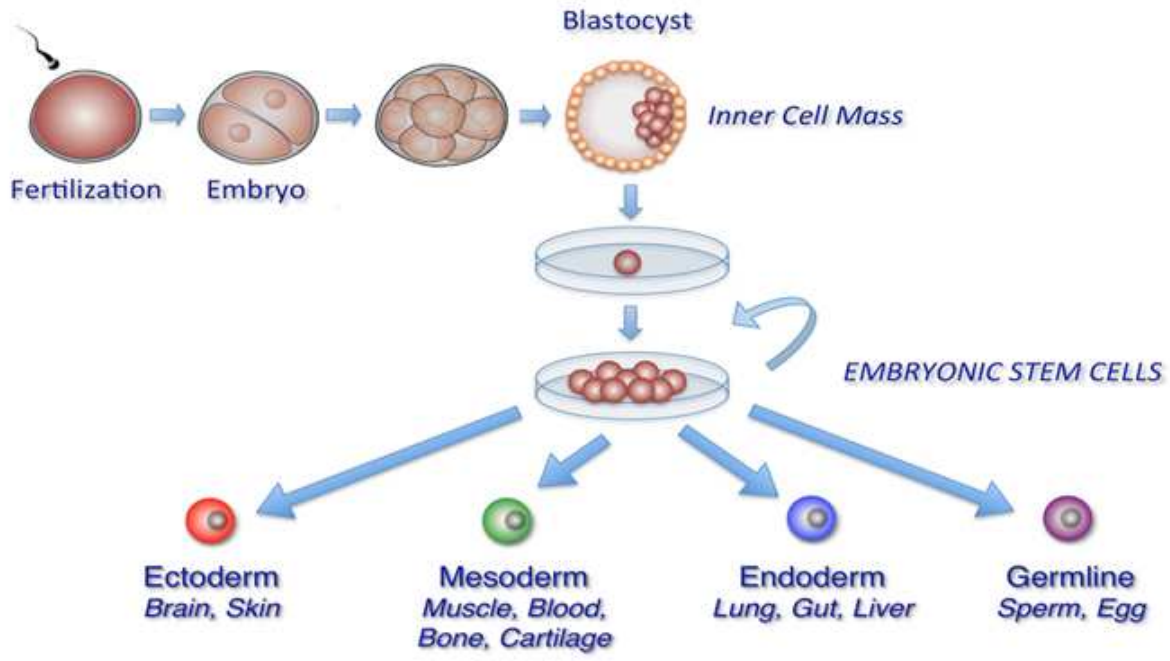

Figure 2: Schematic representation of the isolation of ESCs: the blastocyst contains three components (the inner cell mass, the trophoblast and the blastocoel); ESCs are isolated from the inner cell mass of blastocysts and form all the tissues of the body; the three germ layers (mesoderm, ectoderm and endoderm) are formed during gastrulation (Yabut and Bernstein, 2011; edited by Wegener).

Although these pluripotent cells are relatively short-lived in the embryo *in vivo*, they have the ability to stay in an undifferentiated state *in vitro* by growing in the presence of leukemia inhibitory factor (LIF) and/or on a feeder layer of murine embryonic fibroblasts (MEF) (Smith et al., 1988; Williams et al., 1988; Rippon and Bishop, 2004; Kawahara et al., 2009). When LIF or

MEF are withdrawn, most types of ESCs differentiate spontaneously to form aggregates formally known as embryoid bodies (EBs) (Kawahara et al., 2009; Hescheler et al., 1997). These spherical structures consist of a range of different cells including cells of all three germ layers and plenty of other cells.

The synchronous formation of EBs can be achieved by removal of the feeder cell layer or LIF followed by suspension culture. EBs recapitulate many aspects of cell differentiation during early embryogenesis. The continuous culturing of murine ESCs *in vitro* as embryoid bodies leads to the formation of a range of differentiated cell types including the three germ layers as well as cardiomyocytes, hematopoietic, endothelial and skeletal muscle cells, neurons as well as chondrocytes, adipocytes, liver and pancreatic islets (Kurosawa, 2007; Kawahara et al., 2009; Hescheler et al., 1997).

1.4 Cardiomyogenesis

A basic approach to study cardiomyogenesis, a process which leads to the formation of the myocardium, is provided by the use of pluripotent murine embryonic stem cells (mESCs) by focusing on the differentiation capability *in vitro* (Hescheler et al., 1997). By culturing ESCs *in vitro* in the absence of LIF or MEF, the cells form embryoid bodies, which consist of a various number of cell types including cardiomyocytes. This multicellular arrangement in EB outgrowth, cardiomyocytes appear as spontaneously contracting cell clusters (from day 7 onwards). During differentiation, these clusters increase in size and the contractions intensity (Hescheler et al., 1997).

There have been several cardiac specific genes detected, which play a crucial role in the development of cardiomyocytes such as α- and β- cardiac myosin heavy chain (myosin heavy chain 6 and 7), atrial natriuretic factor (ANF) and myosin light chain isoform 2V (MLC-2V) (Hescheler et al., 1997). These genes are also involved in EB contractions and can give an

overview of the differentiation status. Furthermore, EBs are transparent due to their small number of cell layers; thus, they can readily be analyzed by light microscopy (Hescheler et al., 1997).

In previous studies the formation and differentiation of cardiomyocytes in EB outgrowth was explored under simulated microgravity as well as under normal gravity conditions. One of the pilot studies were carried out with murine embryonic stem cells under a 1 *g* environment (Shinde et al., 2015). Another study was performed under simulated microgravity conditions (Shinde et al., 2015) to investigate the effect of gravity (simulated microgravity) on differentiation, pluripotency and differentiation markers as well as on genes which are involved in cardiomyogensis (Myh 6, myosin heavy chain 6, and Myh 7, myosin heavy chain 7). There were no studies performed under hypergravity conditions so far, although increased gravitational stimulation - hypergravity - may have an impact on the development of embryonic stem cells and cardiomyocytes, respectively.

1.5 Cell Cycle

The cell cycle is a process in which the replication and transmission of genetic material to daughter cells takes place. Cell cycling consists of two distinct phases, the Interphase and the mitosis (M-phase). The Interphase comprises the G1-, the S- and the G2-phases and prepares cells for mitosis. During the S-phase the chromosome replication takes place, during the M-phase the chromosome transmission occurs, whereas the G1- and G2-phases represent gap phases, which temporarily separate the S- from the M-phase (figure 3). Cells, which are *active* and growing are arranged in the G1-phase and are receptive to signals to begin DNA synthesis. In the S-phase, cells are *actively* replicating DNA. When cells are exiting the S-phase, they start preparing for cell division (mitosis) in the G2-phase and contain twice the normal amount of DNA. Connected to the G2-phase is the M-phase (mitosis), which is a four-step process and consists of the prophase, the metaphase, the anaphase and the telophase and results in cell

division and normal DNA content. In the G0-phase (not shown in figure 3), cells have left mitosis and are quiescent. These resting cells may be reactivated by special signals and enter the G1-phase. After one cell division, each daughter cell starts a new cell cycle beginning in the Interphase with G1.

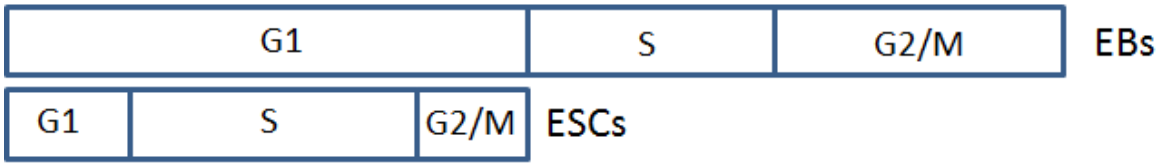

Figure 3: Comparison of the schematic cell cycle structure of embryonic stem cells (ESCs) and embryoid bodies (EBs): M=Mitosis, S=Synthesis (S-phase), G1/G2=Gap phases (from White and Dalton, 2005; edited by Wegener).

White and Dalton (2005) reported that pluripotent cells in the rodent epiblast have an unusual cell cycle structure, in which the cells are devoted to the S-phase and just a few cells formed G1- and G2-gap phases. Furthermore, it has been reported that also other pluripotent populations such as murine embryonic stem cells, human embryonic stem cells, murine embryonal carcinoma and embryonal germ cells show such a cell cycle structure (White and Dalton, 2005).

Figure 4 shows the differences of the cell cycle structures of undifferentiated murine embryonic stem cells (left) in comparison to differentiated cells derived from embryonic stem cells (EBs) (right). Note the prominent change in cell cycle structure accompanying differentiation, particularly the expansion of the G1- and the S-phase. The SubG1-phase, leftmost peak next to the G1-phase, consists of fragmented and apoptotic cells, including nuclear fragmentations, chromatin condensation and DNA fragmentations.

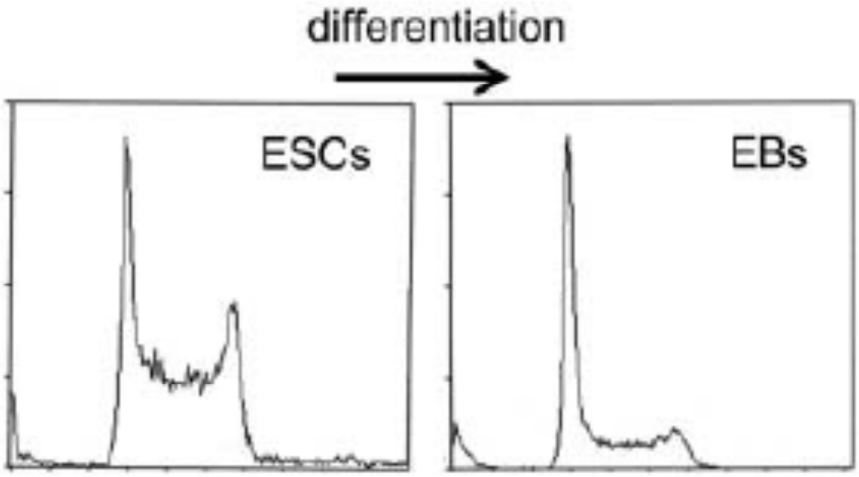

% S-phase	62	13
% G1	21	51
% G2/M	17	26
Cell cycle time (hours)	8-10	> 16

Figure 4: Embryo-derived pluripotent cells have an unusual cell cycle structure. Undifferentiated mESCs (left) and embryoid bodies (EBs) (right) derived from mESCs were stained with propidium iodide (PI) and analyzed by flow cytometry (from White and Dalton, 2005; edited by Wegener).

1.6 The Cytoskeleton in Altered Gravity

The cytoskeleton of eukaryotic cells can have a multitude of functions: on the one hand it gives the cell shape and mechanical resistance to deformation, and on the other hand the cytoskeleton is involved in many signaling pathways and biological processes. Furthermore, it allows cells to migrate and import extracellular material (endocytosis). The cytoskeleton is also responsible in segregating chromosomes during cellular division, and it forms specialized structures such as flagella, cilia and lamellipodia or podosomes (e.g. Crawford-Young, 2006), enabling cell locomotion. The cytoskeleton is composed of three main protein classes, which are capable of

rapid assembly and disassembly (McKinley et al., 2015). This property gives the cytoskeleton its dynamic structure.

Eukaryotic cells such as embryonic stem cells contain three main kinds of cytoskeletal filaments: microfilaments (MF), intermediate filaments (IF) and microtubules (MT). Microfilaments or actin filaments are composed of actin, intermediate filaments are composed of a family of related proteins sharing common structural and sequence features, and microtubules are built with tubulin as the basic subunit.

It has been reported that it can have detrimental effects on individual cells, when parts of the cytoskeleton do not act in a normal fashion (Crawford-Young, 2006). The interactions between microtubules, intermediate filaments, microfilaments and associated proteins are essential for the normal behavior of the cytoskeleton in cells.

At the level of the cell, a number of structural alterations take place under microgravity, especially regarding the cytoskeleton, which becomes disorganized, and in cellular responses to the environment (Crawford-Young, 2006). Changes in the gravitational field affect not just the cell architecture such as the cytoskeleton; they also affect the position of cell organelles like mitochondria and nuclei, which cause an increase in cell apoptosis and the function of cell organelles can be affected as well (Crawford-Young, 2006). Also it has been reported that there are differences in the cell´s morphology under 1 *g* compared to microgravity (Crawford-Young, 2006).

1.7 Aim of this Study

The influence of altered gravity (microgravity and hypergravity) on the development of embryonic stem cells is still not well understood. Shinde et al. (2015) developed a method to expose ESCs to simulated microgravity conditions using the principle of clinorotation. First results indicated that there are changes in the gene expression and the embryoid body morphology. The present study complements the study of Shinde et al. (2015) in terms of cell

cycle and cytoskeleton analysis of clinorotated embryonic stem cells and in studying the effect of hypergravity on ESCs differentiation considering the three germ layers and their derivatives (e.g. cardiomyocytes).

Embryonic stem cells were exposed to simulated microgravity and to a hypergravity environment for indicated time periods and then transferred to petri dishes to investigate possible changes in cell cycle distribution, gene expression, cytoskeleton arrangement, EB morphology and differentiation. Embryoid body “beating” patterns under 1 g and hypergravity were observed as functional read out for cardiomyogenesis.

2 Materials and Methods

2.1 Materials

2.1.1 Consumables

Cell culture dishes (10 cm)	Greiner Bio-one, Solingen, Germany
Cell culture flasks (T25, T75)	Thermo Fisher Scientific, Karlsruhe, Germany and Sarstedt, Nürnbrecht, Germany
40 µm cell strainers	Greiner Bio-one, Solingen, Germany
Cover slips	Roth, Karlsruhe, Germany
Falcon tubes (15 mL, 50 mL)	Roth, Karlsruhe, Germany and Sarstedt, Nürnbrecht, Germany
Pipette tips (10 µL, 200 µL, 1000 µL, 5000 µL)	Roh, Karlsruhe, Germany and VWR, Darmstadt, Germany
Pipettes, plastic, sterile (1 mL, 5 mL, 10 mL, 25 mL, 50 mL)	Roth, Karlsruhe, Germany and VWR, Darmstadt, Germany
Eppendorf tubes (1.5 mL, 2.0 mL)	Eppendorf, Hamburg, Germany and Roth, Karlsruhe, Germany

Slides	Roth, Karlsruhe, Germany
Syringe (1 mL)	Braun, Melsungen, Germany

2.1.2 Reagents

2-Mercaptoethanol	Life Technologies, Darmstadt, Germany
Antibiotic-penicillin-streptomycin	Biochrom, Berlin, Germany
Bovine serum albumin (BSA), fetal bovine serum	Life Technologies, Darmstadt, Germany
DAPI (4',6-diamidino-2-phenylindole)	Applichem, Darmstadt, Germany
Ethanol (EtOH)	Roth, Karlsruhe, Germany
Ethanol absolute	Merck Chemicals, Darmstadt, Germany
Fluorescence Mounting Medium	Dako, Hamburg, Germany
Glasgow´s minimum essential medium	Life Technologies, Darmstadt, Germany
Leukemia inhibitory factor (LIF)	Merck Chemicals, Darmstadt, Germany
Paraformaldehyde (PFA)	Roth, Karlsruhe, Germany
PBS (Phosphate Buffered Saline)	Roth, Karlsruhe, Germany

Polyethyleneimine (PEI)	Sigma Aldrich, Munich, Germany
Phalloidin-Texas Red	Invitrogen, Karlsruhe, Germany
Propidium Iodide (PI)	Thermo Fisher Scientific, Karlsruhe, Germany
Triton X-100	Roth, Karlsruhe, Germany
Trizol	Thermo Fisher Scientific, Karlsruhe, Germany
Trypsin/EDTA	Sigma Aldrich, Munich, Germany

2.1.3 Kits

First Strand cDNA Synthesis kit	Thermo Fisher Scientific, Karlsruhe, Germany
RNeasy mini kit	Quiagen, Hilden, Germany
SYBR-Green PCR Master Mix	Life Technologies, Darmstadt, Germany

2.1.4 Nucleotide Sequences

Table 1: Nucleotide sequences of the primers used for qRT-PCR.

Sr. No.	Gene symbol	Forward	Reverse
1	*Troponin*	5’ CGTGGTCCTGGCTGCTGAGC 3’	3’ CAGCTGGCTGGGGGCTGGAA 5’
2	*Oct 4*	5’ CAGCAGATCACTCACATCGCCA 3’	3’ GCCTCATACTCTTCTCGTTGGG 5’
3	*Klf 4*	5’ CTATGCAGGCTGTGGCAAAACC 3’	3’ TTGCGGTAGTGCCTGGTCAGTT 5’
4	*Cdh 1*	5’ TGATGATGCCCCCAACACTC 3’	3’ TGGCAGTGTCCCTCCAAATC 5’
5	*Nanog*	5´ GCGGACTGTGTGTTCTCTCAGGC 3´	3´ TTCCAFATCCFTTCACCAGATAG 5´
6	*Myh 6*	5’ GCTGGAAGATGAGTGCTCAGAG 3’	3’ TCCAAACCAGCCATCTCCTCTG 5’
7	*β-actin*	5’ GCACCACACCTTCTACAATG 3’	3’ TGCTTGCTGATCCACATCTG 5’

2.1.5 Cell Culture Media

Culture medium for CGR8 (CD-medium): Glasgow´s minimum essential medium with 2 mmol/L glutamine, 50µmol/L β-mercaptoethanol, 1000 units/mL leukemia inhibitory factor (LIF), penicillin (100 units/mL) / streptomycin (100 µg/mL) and 10 % fetal bovine serum.

Random Differentiation Medium (RD-medium): Glasgow´s minimum essential medium with 2 mmol/L glutamine, 100 µmol/L β-mercaptoethanol, 1% non-essential amino acids, penicillin (100 units/mL) / streptomycin (100 µg/mL) and 20 % fetal bovine serum.

2.2. Methods

2.2.1 Cell Culture

Mouse embryonic stem cells, cell line CGR8 (ECACC No. 95011018), originally provided by the Institute for Neurophysiology, University of Cologne, Germany, were maintained within gelatine-coated flasks in standard embryonic stem cell medium (CD-medium) in the presence of leukemia inhibitory factor (LIF) for at least 48 hours to achieve adhesion. Therefore, a T75 cell culture flask was coated with 5 mL of 0.2 % gelatine and incubated for 30-45 min in a CO_2 incubator at 37 °C. The remaining gelatine was removed and the CGR8 cells, which were frozen in fluid nitrogen, were melted and seeded in 12 mL complete medium with 120 µL LIF. After 24 hours the medium was removed and refilled with fresh complete medium and fresh LIF. Figure 5 represents the experimental plan for both exposures: the cells were first exposed to hypergravity or simulated microgravity for indicated time periods (24 hours, 3 days and 6 days). Then, some samples were fixed for direct analyses whereas other samples were transferred to petri dishes until day 10 (only h *g* experiments) for further investigations.

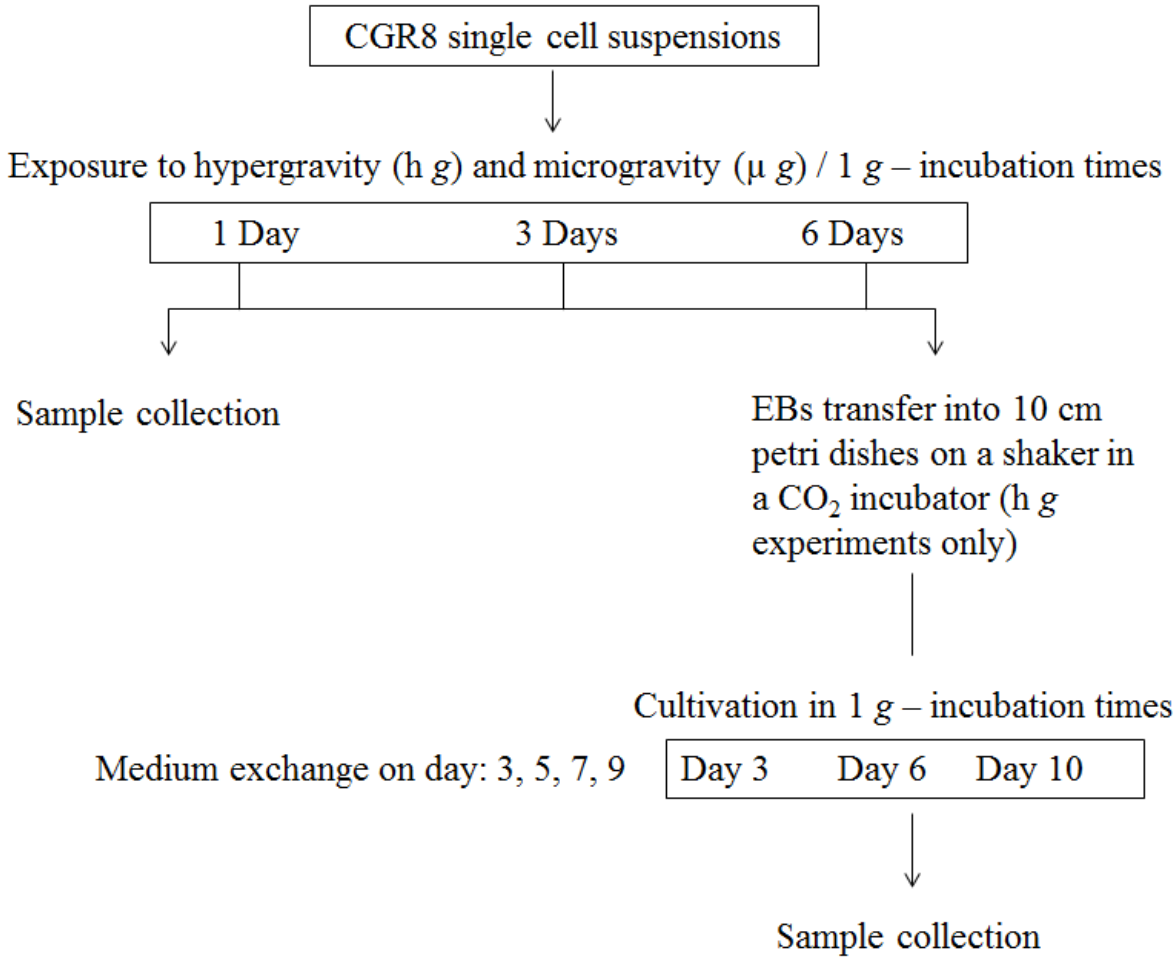

Figure 5: Schematic representation of the experimental plan.

For further processing, the attached cells were collected by trypsinization and the cell numbers were determined by using a Neubauer Chamber (hemocytometer). For trypsinization the medium was removed and the attached cells were washed with 10 mL PBS. PBS was removed and 5 mL 0.05 % trypsin/EDTA (1x) was added and the samples were incubated for 2 min (5 % CO_2, 37 °C). To stop this reaction 5 mL RD medium was added and the cells were transferred to a 15 mL conical tube and centrifuged at 260 *g* for 5 min at room temperature.

2.2.2 Simulated Microgravity Experiments

Microgravity (µ *g*) was generated using the 2D-Pipette-Clinostat (German Aerospace Center, Cologne, Germany) (figure 6) which enables the exposure of non-adherent cells (cell cultures) in 10 (1 mL each) pipettes in parallel. This clinostat was designed and constructed at the German Aerospace Center in Cologne, Germany. Pipettes with a small diameter (3.5 mm) are rotated along their horizontal axis with a speed of 60 rpm resulting in a maximum acceleration of 7 x 10^{-3} *g* at the periphery of the pipettes. The following equation was used to calculate the maximum acceleration:

$$a = \omega^2 \cdot r$$

with a=acceleration, ω=angular velocity, r= radius.

Cultured cells were harvested and the cells were gently resuspended in 5 mL RD medium by pipetting up and down. Mouse embryonic stem cells were counted with a Neubauer Chamber and diluted to a final concentration of 2.5 x 10^4 cells/mL.

The samples were split into two groups: One group in pipettes was cultured at the bottom of the clinostat (static 1 *g* control) and the other group was cultured in the 2D-Clinostat (µ *g* group). The system was placed in an atmosphere of 95 % air / 5 % CO_2 at 37 °C inside an incubator. The day on which the samples were mounted on the clinostat was referred to as day 0.

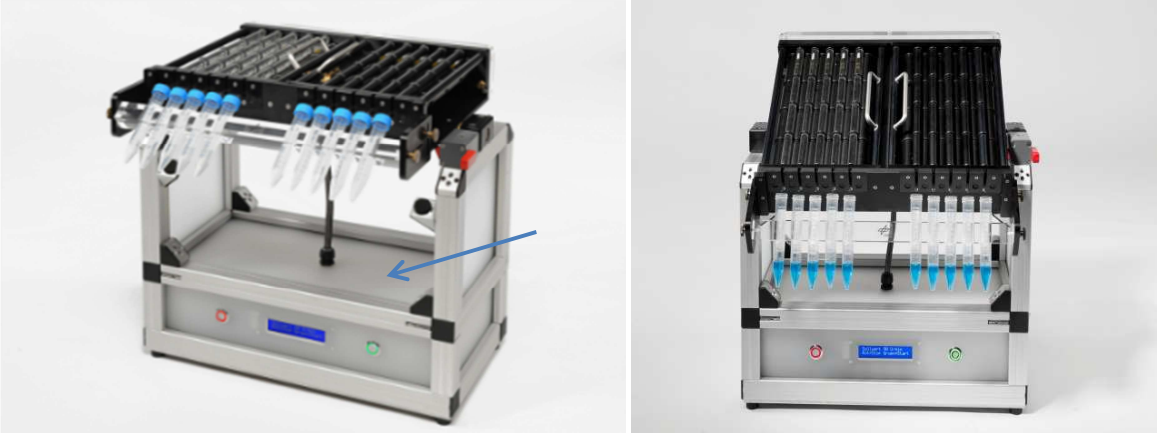

Figure 6: A 2D-Pipette-Clinostat allows the exposure of ten 1 mL pipettes in parallel; 1 *g* controls are located at the bottom (arrow) (DLR, Cologne, Germany; designed by Dr. Jens Hauslage).

700 µL of the cell suspension were transferred to each 1 mL pipette in such a way that the suspension remained in the center of the pipette, thus leaving air at both ends. The openings of the pipettes were closed with sterile parafilm and the pipettes were fixed in the clinostat for various time periods. The treatment (µ *g*) group was rotated and the control (1 *g*) group was kept stationary. For each group 10 pipettes were used. After 1,3 and 6 days two samples from each condition (1 *g* and µ *g*) were collected in 15 mL tubes and centrifuged at 260 *g* for 5 min, afterwards the supernatant was removed and the pellet was rinsed with PBS to prepare the cells for the different fixations.

At day 3 of exposure the medium of all pipettes was changed. Therefore, the cell suspensions of each group (µ *g*, 1 *g*) were transferred to a 15 mL tube and centrifuged at 260 *g* for 5 min, the supernatant was removed and the pellet was gently resuspended in fresh random differentiation medium. New pipettes were aspirated as described above and kept on the rotating clinostat (µ *g*) and at the bottom (1 *g*) until day 6. The experiments were performed three times (n=3).

2.2.3 Embryoid Body Collection and Further Processing

Embryoid bodies (EBs) were collected after 1, 3 and 6 days. For EB collection, the pipettes were removed from the incubator and transferred to a biosafety cabinet. The parafilm was gently removed, and for each condition (1 *g*, µ *g*) two pipettes were inverted inside 1.5 mL sterile Eppendorf tubes. The EBs were centrifuged at 2.2 *g* for 5 minutes at room temperature, the supernatants were aspirated and the EBs were washed twice with 0.8 mL of PBS. Then, the EBs were fixed in 0.8 mL of 4 % PFA for 30 min at room temperature and were washed with PBS again. The Eppendorf tubes were stored at 4 °C for the cytoskeleton staining.

Two pipettes of each condition were transferred to 15 mL conical tubes for flow cytometry analysis. First the EBs were centrifuged at 260 *g* for 5 minutes and washed with PBS as described above. PBS was removed and 1 mL trypsin/EDTA was added to each tube, which were labeled with an A, and incubated for 5 min inside an incubator. After gently pipetting up and down the EBs were centrifuged at 260 *g* for 5 min. The supernatants were transferred to a second 15 mL conical tube (labeled B) and 5 mL random differentiation medium was added. Another 1 mL trypsin/EDTA was added to falcon tubes (labeled A) and incubated for 5 min inside an incubator, then transferred to tubes (labeled B). 40 µm cell strainers were placed on the top of 50 mL conical tubes and the cell suspensions in falcon tubes B were filtered through the strainer kept on 50 mL tubes. The collected filtrates in 50 mL falcon tubes contained single cells and were centrifuged at 770 *g* for 5 min. Supernatants were gently removed, and the pellets were resuspended in 1.5 mL PBS and fixed in 4.5 mL of ice cold 100 % EtOH to generate a final concentration of 70 % EtOH. The cell suspensions were stored at -20 °C for at least 24 hours for flow cytometry analysis.

2.2.4 Hypergravity Experiments

Hypergravity was generated using the Multi Sample Incubator Centrifuge (MuSIC, DLR, Cologne, Germany), which was placed in an incubator at 37 °C and 5 % CO_2 (figure 7). Confluently grown CGR8 cells from T75 cell culture flasks were trypsinized and transferred to T25 cell culture flasks with a final concentration of 2.5 x 10^4 cells/mL and a total volume of 25 mL. Mouse embryonic stem cells were exposed to a continuous hypergravity (h *g*) of 1.8 *g* (with a speed of 100 rpm) for 1, 3 and 6 days. The 1 *g* controls were grown in parallel in T25 cell culture flasks at the bottom of the centrifuge in the same incubator. The day on which the cells were mounted on the centrifuge was referred to as day 0. All experiments under hypergravity conditions were performed four times (n=4).

At day 3 of exposure the medium was changed. Accordingly, the EB suspensions of the treatment and the control group (h *g*, 1 *g*) were transferred to a 50 mL tube and centrifuged at 260 *g* for 5 min, the supernatants were removed and the pellets were gently resuspended in 25 mL of fresh random differentiation medium. The same flasks were used and refilled.

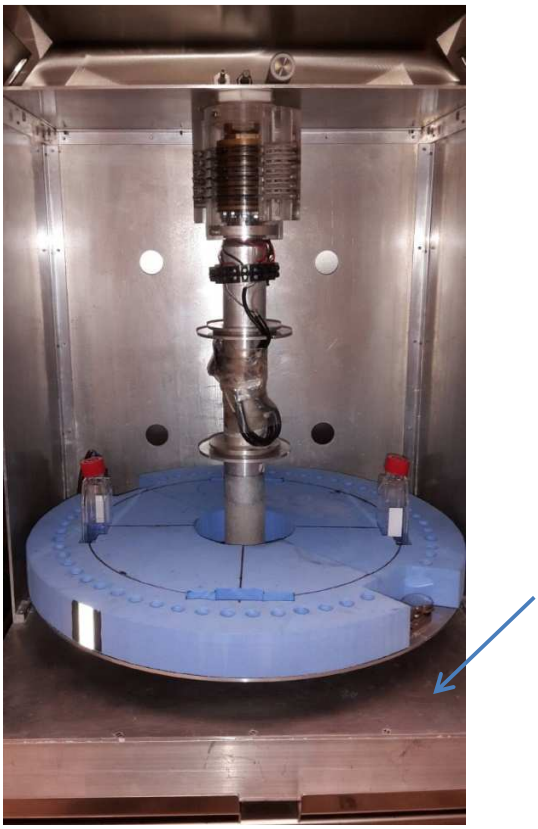

Figure 7: Multi Sample Incubator Centrifuge: for incubation during hypergravity conditions of cell cultures different inserts have been constructed. Depending on the experimental demands, accelerations up to 40 *g* under controlled environmental conditions can be applied. 1 *g* controls are located at the side of the centrifuge (arrow) (DLR, Cologne, Germany).

2.2.5 Embryoid Body Collection and Further Processing

For EB collection the cell culture flasks were removed from the incubator to a biosafety cabinet and inverted to 50 mL falcon tubes. Then for each condition (1 *g*, h *g*) 3 mL of CGR8 EBs were transferred to petri dishes (10 -cm diameter) containing 12 mL of RD medium. These CGR8 EB-containing dishes were placed on a continuously shaking device inside a CO_2 incubator (reciprocation motion 50/min) until day 10. The medium was changed every second day.

On day 3, 6 and 10 the EBs from the petri dishes were collected and fixed in Trizol. Trizol is a reagent, which can be used for the isolation of high-quality total RNA, DNA and protein of biological samples such as embryonic stem cells. Therefore, the EBs were washed with 2 mL of PBS twice and collected in 1 mL Trizol, transferred into 1.5 mL DNAse free tubes and stored at -80 °C until RNA isolation. Right after the exposure to hypergravity EBs were also collected in 1 mL Trizol after 1, 3 and 6 days. The petri dishes were photographed (stereomicroscope Nikon SZM 1500, Nikon Instruments Europe B.V., Germany) at the collection days to analyze the EB morphology (diameter, area and circularity).

Furthermore, 1.5 mL of the EB suspensions (1 *g*, h *g*) were fixed in 0.8 mL of 4 % PFA for cytoskeleton staining as well as for flow cytometry analysis as described for the microgravity experiments.

2.2.6 Cytoskeleton Staining (Phalloidin/DAPI)

After the fixation in PFA the samples of treatment and control groups (h *g*, µ *g*) were centrifuged at 2.2 *g* for 5 min and washed three times with PBS. The supernatants were removed and 400 µL of 1 % Triton-X100 in PBS was added for 2 min at room temperature, followed by three washing steps with 0.1 % BSA in PBS. Subsequently the samples were blocked in 3 % BSA in PBS for 1 hour at room temperature and centrifuged at 2.2 *g* for 5 min. Then Phalloidin-Texas Red (it binds and stabilizes actin polymers) in PBS with a ratio of 1:40 was added to each sample and incubated for 1 hour followed by a centrifugation (2.2. *g*, 5 min) and three washing steps with 0.1 % BSA. In order to stain the nuclei, DAPI (4',6-diamidino-2-phenylindole), which is a fluorescent stain that binds strongly to A-T rich regions in DNA, was added for 20 min in darkness. In the meantime an area of 2 cm in diameter was encircled on 0.1 % PEI (Polyethyleneimine) in PBS coated slides with a pap pen. The samples were rinsed with PBS twice and a drop of EB suspension was transferred to the slides, mounted in DAKO, a mounting

medium for fluorescent microscopy protecting the samples against whitening, and covered. The slides were analyzed by a confocal laser scanning fluorescent microscope (Nikon D Eclipse 80*i*, Nikon Instruments Europe B.V., Germany) and processed with ImageJ (Fiji Is Just, Image Processing and Analysis in Java).

2.2.7 Flow Cytometry

Flow cytometry is a laser-based method measuring the physical and chemical characteristics of cells as they travel past a detector in a single cell suspension. Flow cytometers consist of a light source (laser with a specific wavelength), collection optics, electronics and a computer that translates signals to data. A fine stream of the cell suspension is directed through the laser beam, where every passing cell scatters and absorbs some of the light and might additionally emit fluorescence. A detector in front of the light beam measures forward scatter, which correlates with cell size. Several detectors measure side scatter. Side scatter is proportional to the granularity of the cells. These fluorescence detectors quantify the fluorescence emitted from stained cells or particles (Part, 2000; PD Dr. Hellweg, personal communication).

Flow cytometers can also be used for cell cycle analysis and cell sorting. The most commonly used dye for DNA content and cell cycle analysis is propidium iodide (PI) (Part, 2000; Hellweg, personal communication). Propidium iodide passes through a membrane, intercalates into the major groove of double-stranded DNA and produces a highly fluorescent adduct that can be excited at 488 nm (Part, 2000; Hellweg, personal communication). For cell cycle information see chapter 1.5.

The profile of cells in different phases of the cell cycle was determined using previously established methods (White and Dalton, 2005). After incubation for indicated times (1, 3 and 6

days) cells were processed and stained with PI and then analyzed by FACSCalibur (BD Biosciences, Heidelberg, Germany). For the staining the cell suspensions, which were fixed in EtOH and stored at -20 °C for at least 24 hours, were diluted with PBS at a ratio of 1:1 and centrifuged at 500 *g* for 5 min at room temperature. The supernatants were discarded and 1 mL of PI staining solution was added to each sample and incubated at 37 °C inside a CO_2 incubator for 1 hour.

10 mL PI staining solution contained 10 mL PBS, 500 µL RNA-se, 80 µL propidium iodide and 8 µL Triton-X 100.

The stained samples from the different conditions of simulated microgravity and hypergravity as well as the control groups were then analyzed by a FACSCalibur. All raw data were converted to FlowingSoftware 2.5.1 (a flow cytometry data analysis software) and processed with a programmed analysis for cell cycle phases by PD Dr. Christine Hellweg (DLR, Cologne, Germany) (figure 8). The further analysis was done with Microsoft Excel 2010 (Microsoft Deutschland GmbH), also a special programmed sheet to analyze the different phases of the cell cycle, which was programmed by Prof. Dr. Christa Baumstark-Khan (DLR, Cologne, Germany).

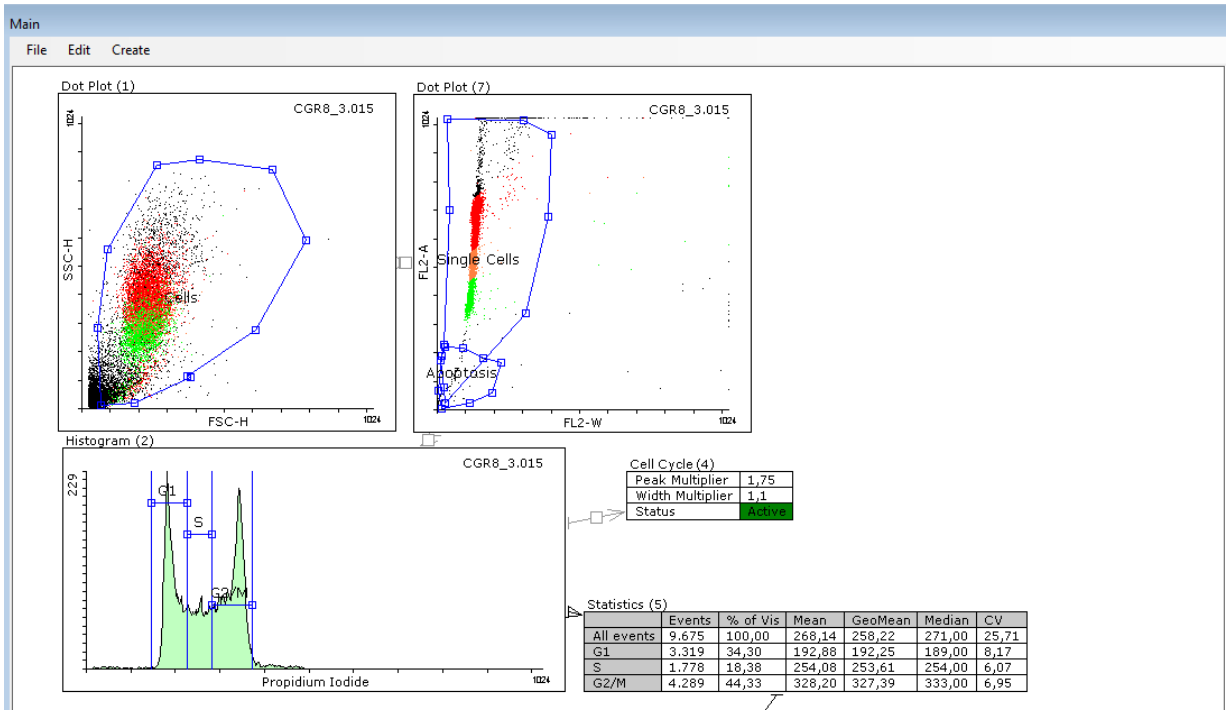

Figure 8: Example of flow cytometry analysis with FlowingSoftware 2.5.1 based on a pilot experiment: The first image (upper left) shows a dot plot of forward and side scatter, below is shown a typical cellular status with the majority of cells in the G0/G1 phase (left peak) and G2/M phase (rightmost peak). The area between these peaks indicates cells within the S-phase. The upper right image shows a dot plot of single cells, below, the statistics are shown. Further analysis can be done with Microsoft Excel.

2.2.8 RNA Isolation and cDNA Synthesis

The isolation and purification of RNA in the course of the hypergravity experiments was performed using an RNeasy mini kit at the Institute for Neurophysiology of the University of Cologne. In brief, the EBs in Trizol were lysed by passing through a 24-G needle with a 1 mL syringe 30 times. 0.2 mL Chloroform ($CHCl_3$) was added, then vortexed to mix the contents uniformly and the samples were centrifuged at 12.500 rpm at 4 °C for 15 min. 400 µL of the top layer, which contained the RNA, was transferred into special filter tubes (which were placed in 1.5 mL collection tubes) and centrifuged for 1 min at 12.500 rpm, then the filter tubes were removed and 450 µL ice cold 100 % EtOH was added to each sample.

These solutions were transferred into special 1.5 mL columns which are used for RNA isolations (RNeasy Mini Spin Columns) and again centrifuged (at 12.500 rpm) for 20 seconds at room temperature. The filtrate was discarded and 600 µL of RW1 buffer (from RNeasy mini kit) was added, followed by a centrifugation for 1 min (at 12.500 rpm). The filtrate was discarded again, then 600 µL RPE buffer (from RNeasy mini kit) was added and the samples were centrifuged once more. Subsequently, the columns were transferred into new 2 mL collection tubes and centrifuged for 2 min at room temperature to remove the buffers completely. The columns were converted to DNase and RNase free 1.5 mL collection tubes and 22 µL nuclease free water was added to the center of the columns for the final 1 min of centrifugation (12.500 rpm). The supernatants contained the RNA. The collection tubes were stored on ice.

The total RNA was purified using an RNeasy mini kit and RNA quantification was performed using NanoDrop 1000 (Thermo Fisher Scientific, Karlsruhe, Germany).

cDNA for the quantitative real-time polymerase chain reaction (RT-qPCR) was then obtained with the First Strand cDNA Synthesis kit. The following protocol has been optimized for generating first-strand cDNA for the use in two-step qRT-PCR. For a single reaction the following components were combined in a tube on ice and gently mixed:

5 X VILO ^{TM} Reaction Mix	4 µL
10 X SuperScriptR Enzyme Mix	2 µL
RNA (up to 2 µg)	x µL
RNase free water to 20 µL	

cDNA First Strand Synthesis conditions were as follows: 10 min at 25 °C, 60 min at 42 °C and 5 min at 85 °C to terminate the reaction.

2.2.9 Reverse Transcriptase Quantitative Real-Time Polymerase Chain Reaction (qRT-PCR)

Quantitative real-time PCR at the Institute for Neurophysiology of the University of Cologne was used to determine the expression levels of the genes of interest (see results and discussion) of the hypergravity (h *g*) experiments. qRT-PCR analysis was performed using an ABI 7500 FAST Detection System (Applied Biosystems). RNA from each sample was reverse transcribed using a SuperScript VILO cDNA synthesis kit (chapter 2.2.8). qRT-PCR was performed for treatment and control group (h *g*, 1 *g*) using SYBR-Green PCR Master Mix. The reaction volume was 20 µL, including 2 µL of template cDNA and a final primer concentration of 500 nmol/L. The Master Mix combined for a single run: 10 µL PlatinumR SYBRR Green qPCR SuperMix-UDG with ROX, 0.5 µL of each Forward and Reverse primer (10 µM) and 7 µL RNase free water.

18 µL of the mixed Master Mix was added to each well on a 96 well PCR plate as well as 2 µL cDNA. Subsequently, the plates were run on the real-time instrument ABI7500 FAST detection system (Applied Biosystems).

PCR conditions were as follows: 2 min at 50 °C, 2 min at 95 °C, 40 cycles of 3 s at 95 °C and 30 s at 60 °C, followed by a melting curve analysis step (15 s at 95 °C, 1 min at 60 °C and 15 s at 95 °C per cycle).

qRT-PCR was performed for the following target genes: Myh 6 (Myosin, heavy chain 6, cardiac muscle), Oct 4 (octamer binding transcription factor 4, pluripotency and differentiation marker), CDH 1 (Cadherin-1, differentiation marker), Klf 4 (Kruppel-like factor 4, differentiation marker), cardiac Troponin (CT, cardiac muscle), Nanog (pluripotency marker).

The gene expressions of target genes were normalized to the housekeeping reference gene β-actin. The relative fold-expression changes were calculated using the algorithm as the power of the negative value of the delta-delta Ct value ($2^{-\Delta\Delta CT}$) with a base of 2 (Livak and Schmittgen, 2001). The resulting mRNA expression values were plotted as a fold change relative to the

respective control with Microsoft Excel 2010 (Microsoft Deutschland GmbH). For raw data analysis the ABI7500 software v2.06 was used.

2.2.10 Embryoid Body Morphology

In a previous study, the morphology of embryoid bodies was investigated under simulated microgravity conditions (Shinde et al., 2015).

In addition to this study, in the present work the EBs were formed by cultivation in a T25 cell culture flask as mentioned in chapter 2.2.5 to analyse the impact of hypergravity on EB morphology. Right after the exposure to hypergravity, the treatment and control group were photographed immediately after 1, 3 and 6 days (stereomicroscope Nikon SZM 1500, Nikon Instruments Europe B.V., Germany, Zeiss Axiovert 10 Inverted Microscope, Carl Zeiss, Oberkochen, Germany) and transferred into petri dishes until day 10. The plates were also photographed at day 3, 6 and 10 to investigate possibly changes in EB morphology. Furthermore, the day on which EBs started “beating” was videographed.

The EBs were photographed at the indicated time points and the diameter, the area and the circularity (roundness, a function of the perimeter and area) were determined using ImageJ and Microsoft Excel 2010 (Microsoft Deutschland GmbH). For circularity the following equation was used:

$$Circularity = \frac{4\,\pi\,Area}{Perimeter^2}.$$

2.2.11 Statistical Analysis

Statistical analyses were performed with GraphPad Prism 5 (GraphPad Software, Inc, USA). Statistics were based on the Kolmogorov-Smirnov normality test. For cell cycle analysis and EB morphology (area, diameter and circularity) Two-way Anova and Bonferroni post hoc tests were performed to evaluate the statistical significance. For qRT-PCR no statistical tests were carried out because of the insufficient mRNA quality and expression values (see results).

A P value of < 0.05 was considered statistically significant. The nomenclature in figures and tables is: * = $p < 0.05$, ** = $p < 0.01$, *** = $p < 0.001$.

3 Results

3.1 Simulated Microgravity Experiments

3.1.1 Macroscopic and Microscopic Observations: Cytoskeleton

In order to study the impact of simulated microgravity on the actin cytoskeleton, three independent experiments were performed with three different passages of CGR8 cells in 1 mL plastic pipettes containing RD medium. For indicated time periods the cells were exposed to simulated microgravity, while the controls were kept at the bottom of the 2D pipette clinostat. At particular time points, EBs were stained with Phalloidin-Texas Red (actin filaments) and DAPI (cell nuclei) to qualitatively investigate visible changes in the formation of actin filaments. In figure 9 the actin filaments and cell nuclei are shown for the specified time periods comparing the treatment (µ *g*) to the control group (1 *g*). The merged pictures as well as the bright field pictures are also represented in figure 9 on the left side. During the observations the microscopy settings (e.g. light intensity) were not changed.

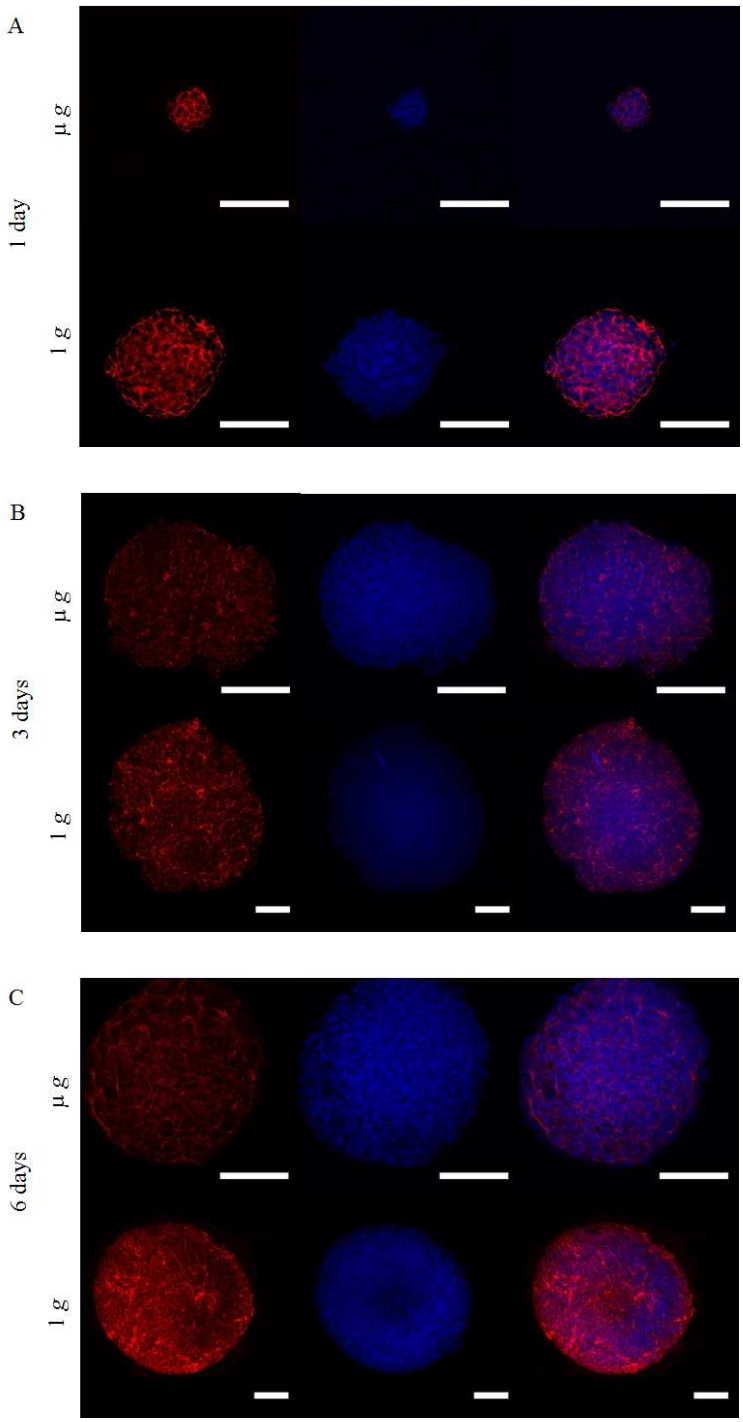

Figure 9: Actin cytoskeleton of cultured embryoid bodies after 1 day (A), 3 days (B) and 6 days (C): comparison of treatment (µ *g*) and control group (1 *g*); EBs were photographed with a confocal laser scanning fluorescence microscope; red: actin filaments (Phalloidin-Texas Red), blue: cell nuclei (DAPI), blue and red: merged. Scale bars: 100 µm.

The 1 day exposure of ESCs to simulated microgravity showed no obvious variations in actin filaments of the resulting EBs compared with the 1 *g* control, though their size differenced as EBs were smaller under simulated µ *g* than the 1 *g* control (figure 9 A). Also the 3 day exposure did not show any sign of change with respect to the actin framework compared with the control group (figure 9 B), whereas on day 6 the microfilaments in clinorotated samples were less pronounced (figure 9 C). The actin framework under 1 *g* condition was denser and tightly arranged compared to the actin framework in cells which had developed in simulated microgravity. There were no obvious changes observed in cell nuclei arrangements after 1 day, 3 days and 6 days between the two gravity conditions. The 6 day control group showed, however, that some cell nuclei were located at the border of the EB, where the actin filaments were diffusely arranged. Furthermore, there were differences in EB sizes observed, especially after 24 hours as well as on day 3 and 6 between the 1 *g* and µ *g* group. The µ *g* samples were smaller than the corresponding control groups (see scale bars figure 9).

3.1.2 Effect of Simulated Microgravity on the Cell Cycle

In order to investigate the effect of simulated microgravity on the proliferation of embryonic stem cells, mouse ESCs were prepared and stained with propidium iodide at different time points during development. Propidium iodide intercalates into the major groove of double-stranded DNA and produces a highly fluorescent adduct. Supplementary, the cells were stained before the start of the experiment and referred to as day 0. For 1, 3 and 6 days, the experiments were performed three times. In figure 10 the differences of the cell cycle structure of undifferentiated murine embryonic stem cells (left) in comparison to embryoid bodies (right) under normal 1 *g* environment, is shown. Note the dramatic change in cell cycle structure accompanying differentiation, particularly the expansion of the G1- and the S-phase. Furthermore, the total number of cells is higher on day 6 than on day 0 (figure 10).

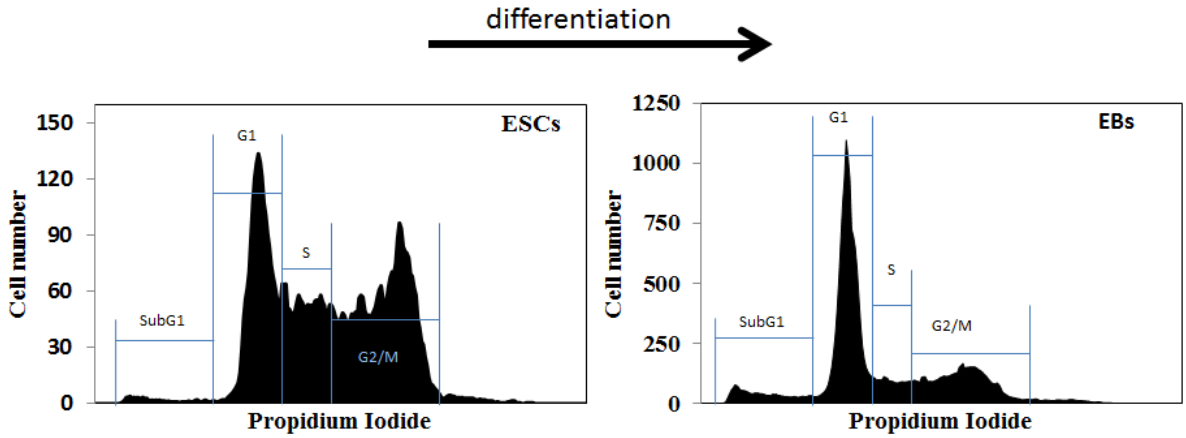

Figure 10: Comparison of cell cycle structure of undifferentiated mESCs (left) and embryoid bodies (EBs) (right) derived from mESCs, which were stained with propidium iodide (PI) and analyzed by flow cytometry.

Figure 11 represents CGR8 cells in different cell cycle phases, which have been maintained in a 1 *g* environment compared to cells kept at simulated microgravity during differentiation until day 6. Here it is shown that most cells were arranged in the G1-phase and that apoptosis (SubG1-phase) was increased during differentiation under 1 *g* as well as under simulated µ *g* conditions (leftmost peak next to G1-phase) compared with undifferentiated cells. This phase consists of fragmented and apoptotic cells, including nuclear fragmentations, chromatin condensation and DNA fragmentations.

Furthermore, in both groups, fewer cells were arranged in the S-phase as well as in the G2/M-phase during development until day 6 compared with undifferentiated cells (figures 10 and 11). When ESCs were maintained at a 1 *g* environment the total number of cells was higher compared with the treatment group at each time point (figure 11).

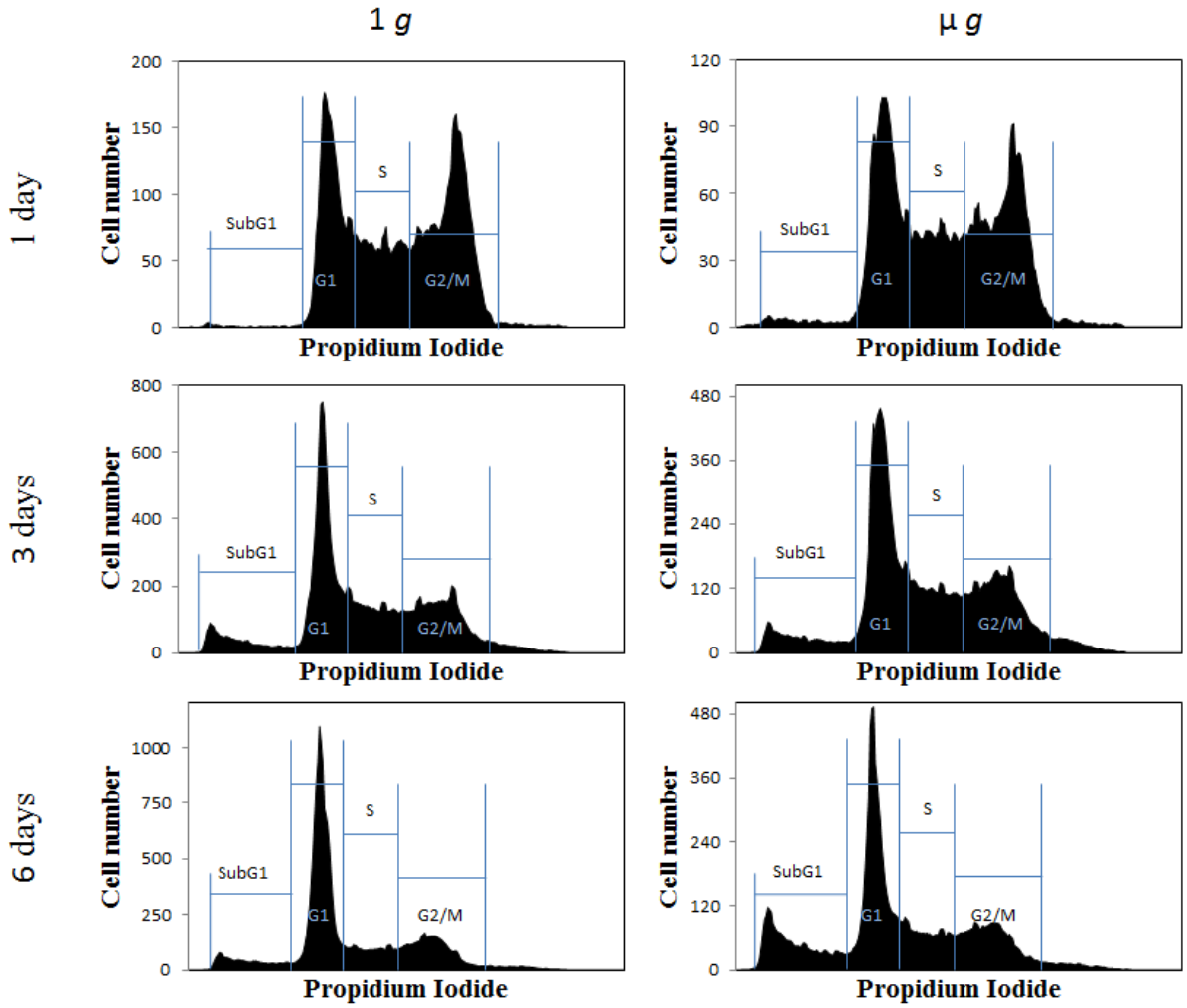

Figure 11: Embryoid bodies derived from mESCs were stained with PI and analyzed by flow cytometry: comparison of cell cycle structure in CGR8 EBs, which were cultured in normal gravity (control group: 1 *g*) and simulated microgravity (treatment group: μ *g*) for different time periods. The data represent means of three experiments (n=3).

Table 2 shows the results of cell cycle analysis and represents the average (in percent) of cells in the different phases of the cell cycle comparing the treatment group (μ *g*) with the control group (1 *g*). There were no significant difference in cell cycle phases between the treatment and control group, except for the G1-phase on day 6 of exposure ($p < 0.001$).

Table 2: Mean percentage of cells in the different cell cycle phases during the exposure to simulated microgravity compared with the 1 *g* controls. Statistical significance (p<0.001) is marked with a *.**

Time points [days]	G1		G2		S		SubG1		Polyploid	
	µ *g*	**1 *g***	**µ *g***	**1 *g***	**µ *g***	**1 *g***	**µ *g***	**1 *g***	**µ *g***	**1 *g***
0	25.4		42		30.7		1.3		0.5	
1	31.6	29.7	38.9	40.2	26.6	29	0.88	2.37	0.6	0.2
3	29.8	31.4	35.6	34.7	24.9	23.6	10.2	9.28	0.5	0.2
6	32.0	44.4***	28.7	27.8	18.8	14.4	13.3	19.2	1.4	0.2

3.2 Hypergravity Experiments

3.2.1 Embryoid Body Morphology and "Beating" Activity

Four independent experiments were performed with four different passages of CGR8 cells in T25 cell culture flasks containing RD medium. For particular time periods the cell culture flasks were exposed to hypergravity, while the control flasks were kept at the bottom of the centrifuge under 1 *g*. Visual observation was performed after transferring EBs into petri dishes and immediately after exposure.

Right after the incubation times, EBs were photographed comparing the 1 *g* control and treatment (h *g*) group. Figure 12 shows that EBs during development in hypergravity conditions built hyphae-like or dumbbell-shaped structures on day 1 and 3. On day 6 of exposure, EBs formed globular chains. The control group had oval EB shapes and differed in EB sizes during further differentiation.

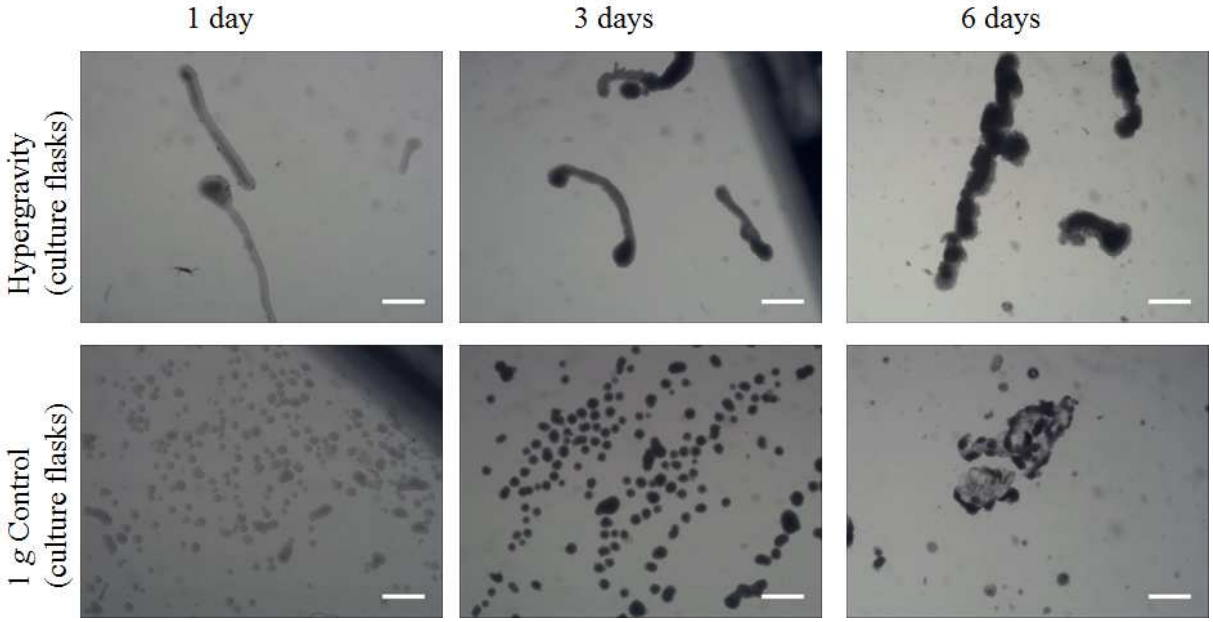

Figure 12: Morphological changes of cultured mESCs and EBs of CGR8 on days 1, 3 and 6 immediately after the exposure to hypergravity (1.8 *g*) in comparison to the control condition (1 *g*) in cell culture flasks. EBs were photographed with the stereomicroscope; scale bars: 1000 µm.

A second control experiment was performed, in which CGR8 cells were cultured in T25 cell culture flasks in 1 *g* until day 6 in the same incubator. Here, the flasks were kept at the bottom of the centrifuge without running any samples on the centrifuge; therefore the cells were not influenced by possible side effects, such as vibrations (figure 13). These cells showed the formation of cell spheres (EBs) with a clear round shape and a more or less equal size.

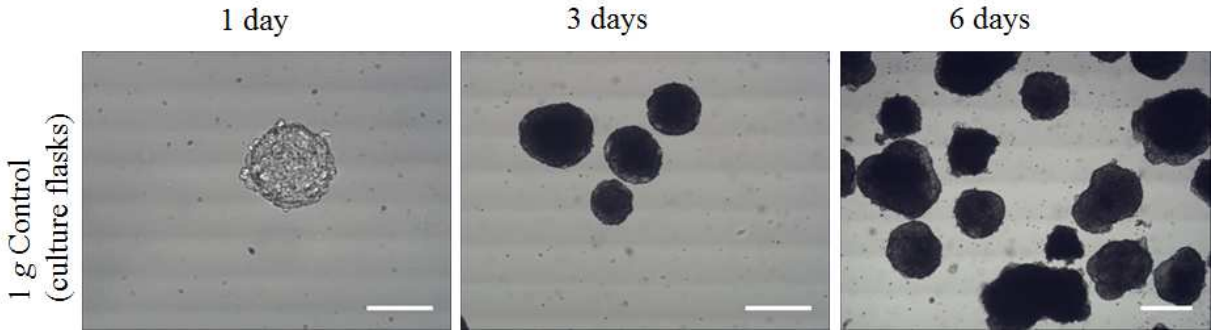

Figure 13: Morphological changes of cultured mESCs and EBs of CGR8 on days 1, 3 and 6 under 1 *g* conditions. EBs were photographed with the stereomicroscope; scale bars: 1 day: 100 µm; 3 days: 200 µm; 6 days: 300 µm.

3.2.1.1 Changes in the Morphology of Embryoid Bodies

For further processing, EBs were transferred into petri dishes on a shaker and further cultivated under similar conditions (incubator: 37 °C, 5 % CO_2, 95 % air) until day 10. These EBs showed the capability to reorganize their EB shape and were able to form structures similar to EBs under the 1 *g* environment at each time point (figure 14). Furthermore, EBs showed a slightly "damaged" shape on each time point after transfer into petri dishes.

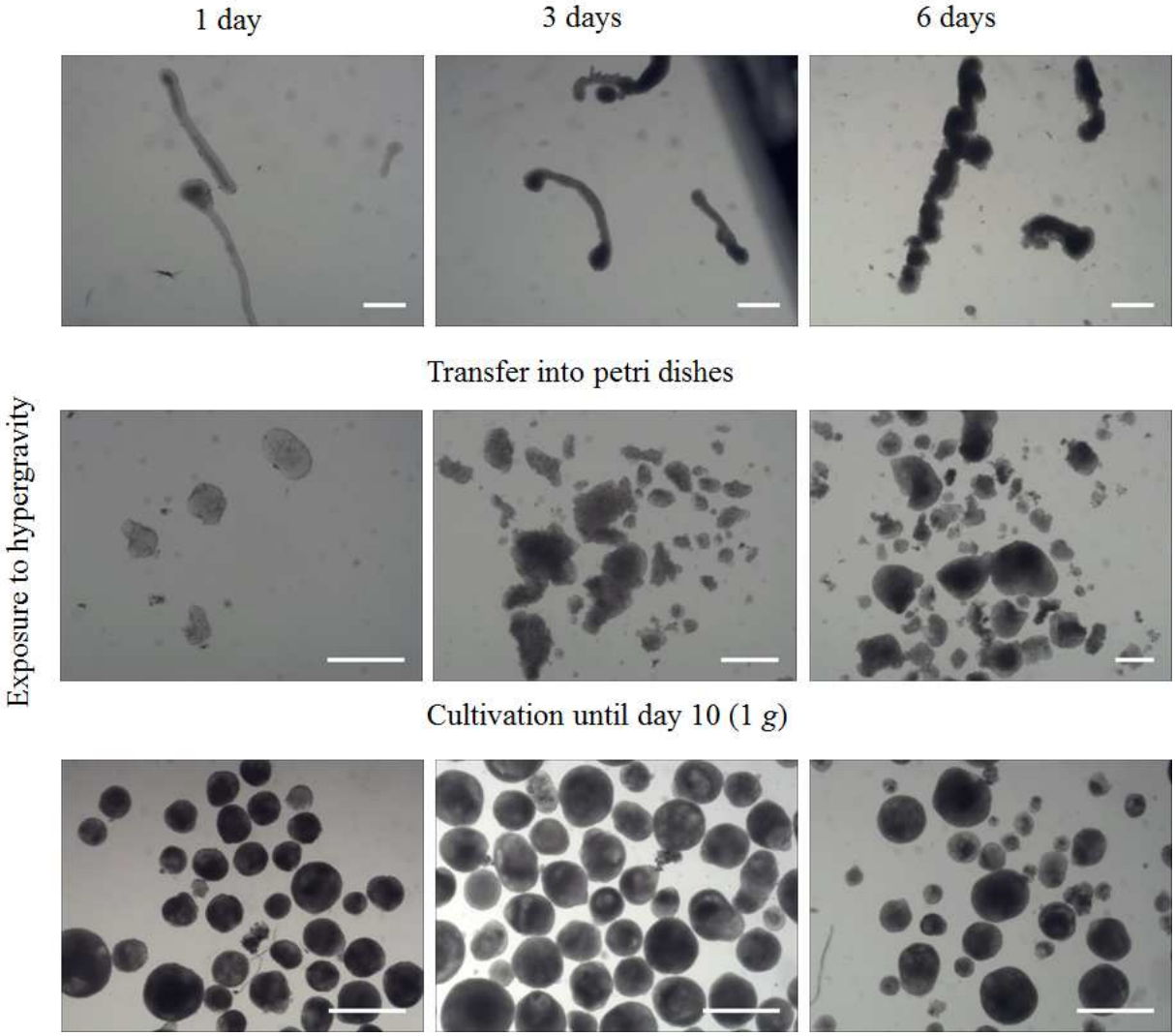

Figure 14: Embryoid body reorganization: cells were exposed to hypergravity (1.8 *g*) for 1, 3 and 6 days and transferred into petri dishes until day 10 (central row). Within this timespan EBs reorganized their cell shape (bottom raw). EBs were photographed with the stereomicroscope. Scale bars: 1000 µm.

Furthermore, microscopic observations of EBs at 1 *g* and at hypergravity conditions revealed that EBs formed under the influence of hypergravity were significantly larger in area (1 day: $p < 0.05$, 6 days: $p < 0.001$) and in diameter (24 hours: $p < 0.05$, 6 days: $p < 0.01$) than those formed in 1 *g* at 1 day and 6 days, when EBs were observed right after the exposure (figure 15 A, B). On day 3 of exposure EBs had a smaller area and diameter than after 24 hours and 6 days. During the

development under normal gravity conditions, the diameter of embryoid bodies was more or less constant. Regarding circularity, no significant differences were observed (figure 15 C); the circularity factor ranged between 0.58 and 0.7 for both, hypergravity and 1 *g* condition.

For comparison, the mean circularity factor of embryoid bodies under normal 1 *g* conditions was 0.82 after 1 day, after 3 days it was 0.86 and 0.8 after 6 days, which reflects the specific round EB shapes (data not shown).

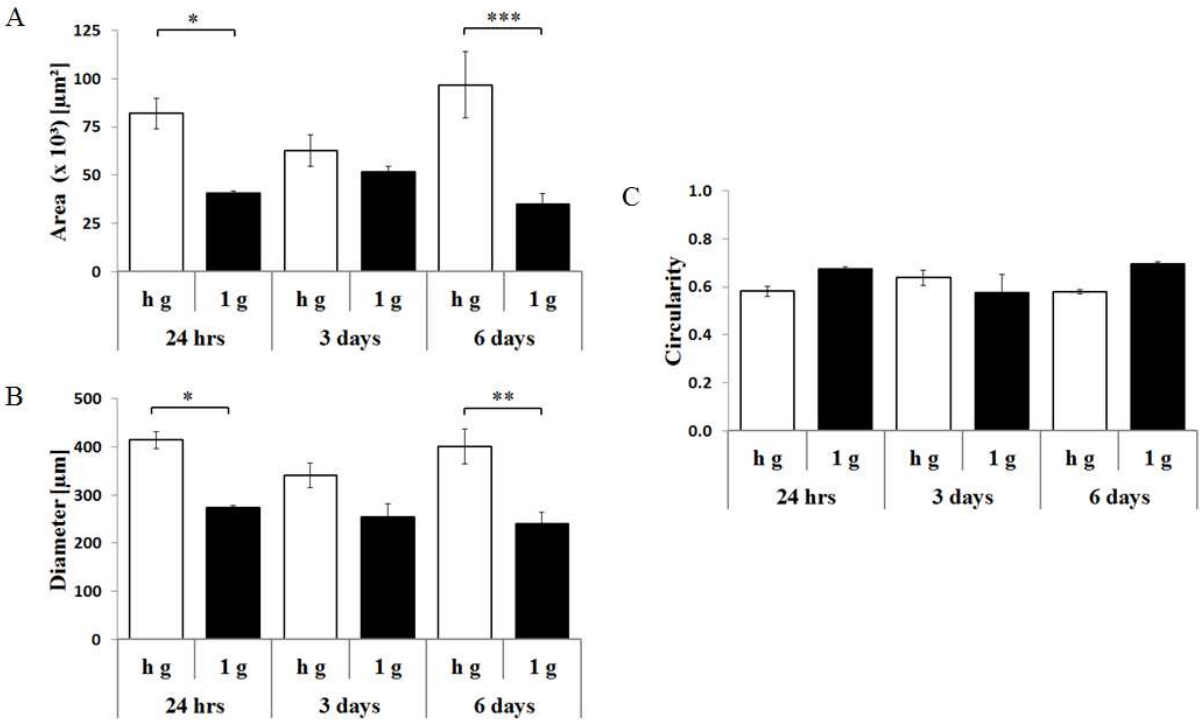

Figure 15: Morphological changes in area (A), diameter (B) and circularity(C) after incubation of ESCs under hypergravity or 1 *g* for different time periods in cell culture flasks. The data represent means ± standard errors of four independent experiments (n=4).

3.2.1.2 Embryoid Body "Beating" Activity

The exposure of cells to hypergravity resulted in the formation of hyphae like structures of EBs as compared with those formed in the 1 *g* control (figure 12). These EBs, when transferred to petri dishes on a shaker, reorganized their usual EB shape and formed structures similar to EBs under the 1 *g* environment (figure 14). Furthermore, they differentiated into a variety of cell types including cardiomyocytes, which are able to contract. These EB containing plates were further observed as functional read out for cardiomyogenesis until day 10. EBs, when exposed to hypergravity for 24 hours, started "beating" on average at day 6.75 under 1 *g* and on average at day 7.5 under hypergravity conditions (n=4). The 3 day as well as the 6 day hypergravity exposed samples were transferred to petri dishes until day 10 as well and showed increased beating patterns compared with the control group. EBs, when exposed to hypergravity for 3 days (n=4), started "beating" on average at day 7.5, whereas the control group started "beating" on average at day 9.3. The 6 day exposure (n=4) resulted in EBs starting their "beating" on average at day 7.5; in contrast, EBs at 1 *g* started "beating" on average at day 10.

3.2.2 Microscopic Observations: Cytoskeleton

For microscopic observations of the cytoskeleton of embryonic stem cells, four independent experiments were performed with four different passages of CGR8 cells in cell culture flasks containing RD medium. At the indicated time periods (24 hours, 3 days and 6 days) samples were collected and EBs were stained with Phalloidin-Texas Red (actin filaments) and DAPI (cell nuclei). During the observations the illumination conditions were not changed.

In figure 16 the actin filaments and cell nuclei are shown for the indicated time points comparing the treatment (h *g*) with the control group (1 *g*). The samples exposed to hypergravity for 1 day (**A**), 3 days (**B**) and 6 days (**C**) exhibited a strong and tightly arranged actin framework with a high density of actin filaments compared with the corresponding control. Especially on day 3 of exposure, actin filaments had developed from the lower corner to the center of the EB, whereas the actin filaments under 1 *g* were not formed as intense as under h *g*. There were no qualitative changes observed in cell nuclei between the different conditions.

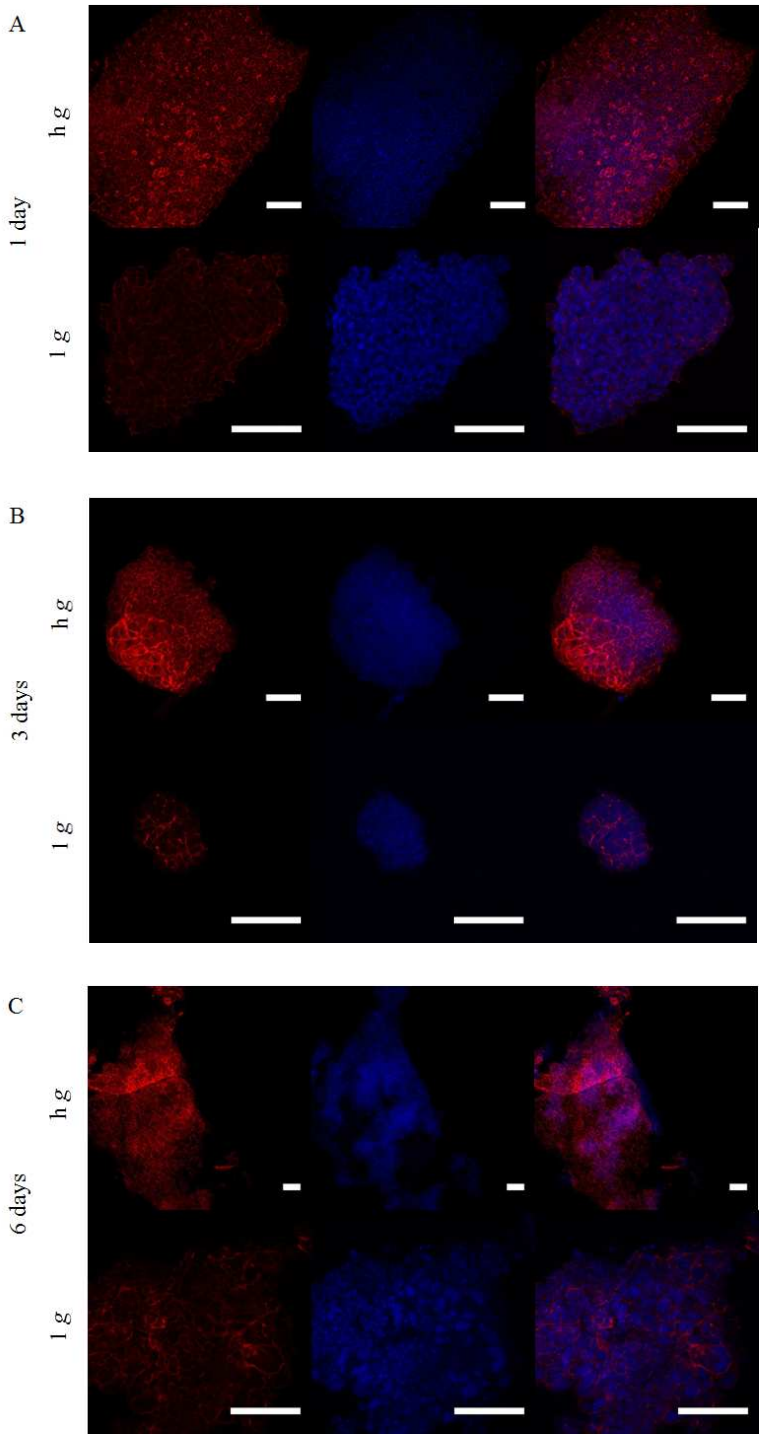

Figure 16: Cytoskeleton of cultured embryoid bodies after 1 day (A), 3 days (B) and 6 days (C): comparison of treatment (h *g*) and control group (1 g); EBs were photographed with a confocal laser scanning fluorescence microscope; red: actin filaments (Phalloidin-Texas Red), blue: cell nuclei (DAPI), blue and red: merged. Scale bars: 100 µm.

3.2.3 Effect of Hypergravity on the Cell Cycle

The effect of hypergravity on cell proliferation was investigated by using CGR8 mouse embryonic stem cells, which were prepared and stained with propidium iodide at indicated time points. Samples were collected after 1, 3 and 6 days of exposure (n=4). The average of the percentage of cells in the different cell cycle phases of four independent experiments was used for further examinations. The cells were stained before the start of the experiment, which was referred to as day 0 (n=4).

Figure 17 represents the adjustment of cells in different cell cycle phases during exposure to hypergravity until day 6. Here, it is shown that most cells were arranged in the G1-phase and that apoptosis (SubG1-phase) was increased at day 3 onwards under 1 g as well as under hypergravity conditions. In both groups, fewer percent of cells were arranged in the S-phase as well as in the G2/M-phase during further differentiation. Note the dramatic decrease of total cell numbers, when ESCs were exposed to hypergravity compared with the corresponding 1 *g* control groups at each condition.

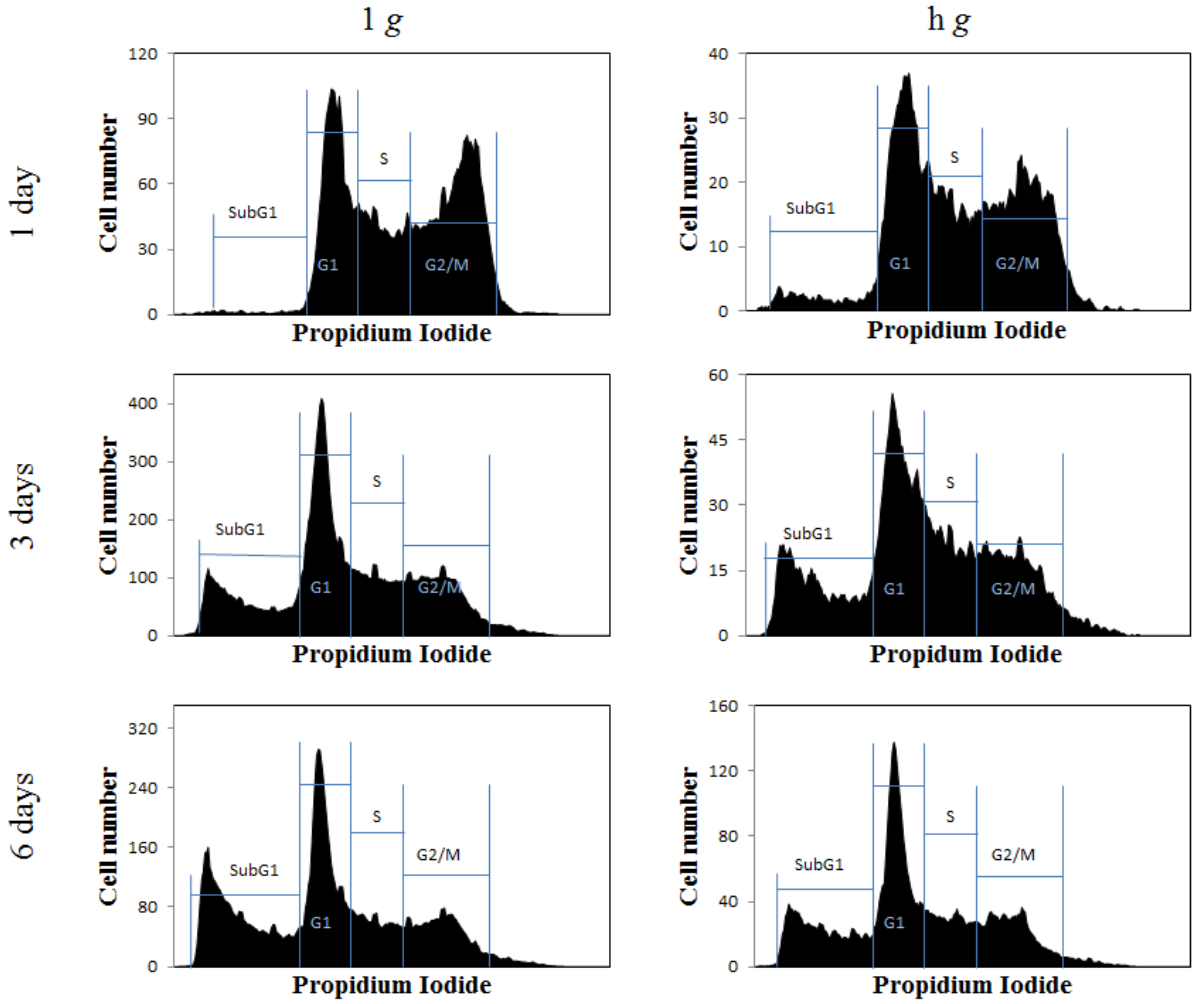

Figure 17: Embryoid bodies derived from mESCs were stained with PI and analyzed by flow cytometry: comparison of cell cycle structure in CGR8 EBs, which were cultured under normal gravity conditions (control group: 1 *g*) and hypergravity (treatment group: h *g*) for different time periods. The data represent means of four independent experiments (n=4).

Table 3 shows the results of the cell cycle analysis and represents the mean percentage of cells in the different phases of the cell cycle comparing the treatment group (h *g*) with the control group (1 *g*). No significant changes were observed during the exposure to hypergravity compared with 1 *g* controls. Noticeable is the strong increase of cells in the SubG1-phase with time, which is also represented in figure 18 (leftmost peak next to G1-phase). Cell numbers in the G2- and S-phase

were decreased with further differentiation, whereas cells in the G1-phase were increased under the normal gravity environment compared with undifferentiated cells (day 0) and cells, which were exposed to hypergravity. There were fewer cells arranged in the G1-phase on day 6 of exposure. Overall, there were no significant differences observed.

Table 3: Mean percentage of cells in the different cell cycle phases during the exposure to hypergravity (h *g*) compared with the 1 *g* control.

Time points [days]	G1		G2		S		SubG1		Polyploid	
	h *g*	**1 *g***	**h *g***	**1 *g***	**h *g***	**1 *g***	**h *g***	**1 *g***	**h *g***	**1 *g***
0	22.9		38.6		37		1.8		0	
1	24.9	26.6	37.5	37.3	32.8	34.4	4.6	1.6	0.2	0.2
3	22.3	24.9	27.2	27.3	28.8	25.4	21.4	22.4	0.3	0
6	17.7	24.2	27.4	24.6	21.1	22	29.2	29	4.5	0.1

3.2.4. Comparison of Cell Cycle Distribution of the two 1 *g* Control Groups

In table 4 the cell cycle distribution of the two 1 *g* controls (1 *g* control of the simulated microgravity experiment vs. 1 *g* control of the hypergravity experiment) is shown. They differ with respect to their location: the 1 *g* control of the simulated microgravity experiments were located at the bottom of the used clinostat (see figure 6), whereas the 1 *g* controls of the hypergravity experiments were located next to the running centrifuge (see figure 7). There were significant changes observed in each cell cycle phase except of the cells, which were polyploid (not shown).

Table 4: Mean percentage of cells in the different cell cycle phases of the two 1 *g* control conditions. Statistical significances are indicated as follows: * (p<0.05), ** (p<0.01), * (p<0.001).**

time points [days]	1 *g* controls									
	G1		G2		S		SubG1		Polyploid	
	h *g*	µ *g*	h *g*	µ *g*	h *g*	µ *g*	h *g*	µ *g*	h *g*	µ *g*
0	22.6	25.4	38.6	42	37	30.7	1.8	1.3	0.03	0.5
1	26.6	29.7	37.3	40.2	34.4	29	1.6	2.4	0.2	0.2
3	24.9	31.4	27.3	34.7*	25.4	23.6	22.4	9.3**	0	0.2
6	24.2	44.4***	24.6	27.8	22	14.4**	29	19.2*	0.1	0.2

3.2.5 Effect of Hypergravity on the Gene Expression

qRT-PCR was performed to quantify the expression levels of the genes of interest (Myh 6, CDH1, Klf4, CT, Nanog, Oct4), which play a crucial role in differentiation, pluripotency and cardiomyogenesis. The gene expressions of target genes were normalized to the housekeeping reference gene β-actin. The relative fold-expression changes were calculated and summarized in table 5. The control values were always 1 for the 1 *g* condition and are not shown in the table.

As a result of the insufficient mRNA quality, one experiment was excluded before qRT-PCR was performed. Furthermore, no statistical analyses were carried out because of the fluctuating expression values of all target genes, which ranged from e.g. 1.4 to 377.2 in the same condition (not shown). In table 5 the mean fold change expression values of all target genes with standard deviations are shown (n=3), which represent the strong variance of the data.

Table 5: Mean fold-expression values of pluripotency and differentiation markers as well as mean fold-expression values of genes involved in cardiomyogenesis ± standard deviations (SD).

cardiomyogenesis			pluripotency markers	
	cardiac Troponin	Myh 6	Nanog	Oct 4
day	mean ± SD	mean ± SD	mean ± SD	mean ± SD
1	35.23 ± 51.74	40.24 ± 64.37	134.39 ± 210.56	4.56 ± 3.87
3	8.59 ± 8.42	1.23 ± 1.06	15.14 ± 21.28	0.74 ± 0.82
6	3.92 ± 5.04	4.87 ± 4.46	5.61 ± 4.61	5.94 ± 5.89

differentiation markers			
	CDH 1	Klf 4	Oct 4
day	mean ± SD	mean ± SD	mean ± SD
1	0.87 ± 0.70	12.41 ± 18.15	4.56 ± 3.87
3	13.09 ± 20.97	3.00 ± 4.48	0.74 ± 0.82
6	1.92 ± 2.60	3.22 ± 4.14	5.94 ± 5.89

The fold-expression values of the target genes relative to the corresponding control (which is 1) showed a strong variance on day 1, day 3 and also on day 6. When embryonic stem cells were exposed to hypergravity, the fold-expression values of e.g. Nanog, one of the pluripotency markers, indicated that during exposure to hypergravity the expression of Nanog decreased as well as the expressions of cardiac troponin, Myh 6 and Klf 4, whereas the fold-expression values of CDH 1 showed a higher expression on day 3 than on day 1 and 6. The fold-expression values of Oct 4 showed a higher value on day 1 and 6 than on day 3, which indicated a higher differentiation potential on day 1 and 6 compared to day 3.

4 Discussion

4.1 Simulated Microgravity Experiments

In this study, the effects of simulated microgravity using the 2D clinostat on qualitatively visible parameters of the actin framework of the cytoskeleton and of the cell cycle of murine embryonic stem cells (ESCs) including apoptosis and proliferation were investigated. Shinde et al. (2015) developed the method to expose ESCs to clinorotation. First results indicated that there are changes in the gene expression and embryoid body morphology, when cells were exposed on a 2D clinostat (Shinde et al., 2015) or to real microgravity (Blaber et al., 2015). The present study complements the study of Shinde et al. (2015) in terms of cell cycle and cytoskeleton analysis of clinorotated embryonic stem cells.

4.1.2 Simulated Microgravity affects the Actin Cytoskeleton

It is well known, that changes in the gravitational field (e.g. microgravity) affects cytoskeleton components of rodents such as microtubules (MT), intermediate filaments (IF) and actin filaments (AF) *in vivo* (Crawford-Young, 2006). There were some studies performed to investigate the influence of real and simulated microgravity on microtubules and actin filaments (e.g. Rösner et al, 2006; Nabavi et al., 2011; Uva et al., 2002). The interactions between MT, IF and AF are crucial for the normal fashion in cells (Crawford-Young, 2006). In the present study, the effect of clinorotation on the actin framework in the cytoskeleton of murine embryonic stem cells *in vitro* was examined. The results indicated qualitative changes in the actin filaments, when ESCs were exposed to a 2D clinostat compared with cells maintained at 1 *g* normal Earth gravity. On day 6 of exposure, the actin framework was denser and tightly arranged under 1 *g* as compared with the actin framework under simulated µ *g*. When the influence of the Earthly gravitational vector is neutralized, there is no force anymore affecting the cells; obviously this condition induces the development of a lesser pronounced actin framework. Consequently, the

tasks of the cytoskeleton (e.g. maintaining cell shape, providing mechanical resistance to deformation and supporting some signaling pathways) may be affected as well. These findings are consistent with earlier observations of the impact of gravity (e.g. Rösner et al., 2006; Nabavi et al., 2011; Uva et al., 2002). Uva et al. (2002) found that cytoskeletal components (microtubules and actin filaments) were damaged after 30 min under simulated microgravity and that actin filaments were highly disorganized. Furthermore, they found altered chromatin condensations and DNA fragmentations in the cell nuclei, which resulted in an increased apoptosis rate (Uva et al., 2002). In the present study, there were no quantitative changes in the arrangement of cell nuclei observed, when ESCs were exposed to clinorotation. There should be further investigations performed focusing on the arrangement of cell nuclei during the exposure to a microgravity environment and furthermore with respect to an increased apoptosis rate induced in microgravity (e.g. using a mitochondrial membrane potential assay kit or a homogeneous caspases assay to proof apoptosis). Changes in the cytoskeleton (actin filaments, microtubules as well as intermediate filaments) have been reported in studies conducted on different types of cells such as osteoblastic and glia cells as well as human MCF-7 cells (breast cancer cells). The cytoskeleton was disorganized at the beginning, but after a certain timespan (approximately 3 days), it was reestablished (Guignandon et al., 2001; Uva et al., 2002; Li et al., 2009). Interestingly, these studies used differentiated cells. These findings hypothesize that embryonic stem cells (initially undifferentiated ESCs, used in this study) may not be able to adapt to the microgravity environment immediately but adapt to it during further exposure, indicated by the reestablishment of their actin network. As a consequence, investigations should be performed focusing on the expression of e.g. tubulin and actin to identify the role of these two main protein classes of the cytoskeleton in adapting towards a new gravitational environment.

4.1.2 Effects of Simulated Microgravity on the Cell Cycle

A number of previous studies, which were focused on the impact of microgravity on ESCs using different experimental approaches to achieve simulated microgravity, have shown a variety of

results (e.g. decreased cell numbers, altered adhesion properties, decreased “stemness” and increased differentiation) (e.g. Wang et al., 2011; Wakayma et al., 2009; Buravkova et al., 2008). In contrast, experiments with ESCs in real microgravity obtained in the course of spaceflight showed a decrease in differentiation markers indicating a discrepancy between the applied simulation approach and real microgravity (Blaber et al., 2015). Here it has to be considered that a variety of ground-based facilities to provide simulated microgravity such as clinostats (2D, 3D) and random positioning machines (RPM) as well as magnets for magnetic levitation have been developed; however, these devices use differing physical principles, and, in consequence, they do not necessarily provide functional weightlessness from the perspective of the biosystem employed (Herranz et al., 2013; Brungs et al., 2015). Depending on the experimental setup (e.g. exposing samples in a small/big radius around the rotation axes) it has to be proven, which microgravity simulator is best for the intended experiments. Wang et al. (2011) e.g. found no changes in cell cycle distribution among different time points (1 and 3 days), when embryonic stem cells were exposed to clinorotation using a 3D clinostat. These results are similar to the results of the present study; on day 1 and 3 no significant differences were observed between clinorotated and 1 *g* samples. However, there was a significant difference in the number of cells in the G1-phase between the 1 *g* group and the µ *g* group on day 6, when ESCs were exposed to the 2D clinostat. More cells were arranged in the G1-phase in both groups and were therefore sensitive to signals to initiate DNA synthesis. The fact that the mean percentage of cells in the S-phase was higher on day 3 and 6 in the µ *g* group compared with the 1 *g* group indicates the capability of undisturbed and even extensive proliferation during the exposure to clinorotation. However, differences in the S-phase between the two groups were not significant. Normally, about half of the cells are arranged in the S-phase in undifferentiated ESCs and this is consistent with the well-known characteristics of embryonic stem cells with respect to their ability to proliferate (White and Dalton, 2005; Wang et al., 2011). Earlier studies indicated that ESCs had an increased apoptosis rate during development under simulated microgravity using a 3D clinostat (Wang et al., 2011). In the present study the results of the cell cycle distribution, especially regarding the mean percentage of ESCs in the SubG1-phase, which consists of fragmented and apoptotic cells, was increased during further differentiation in both conditions (1 *g*, µ *g*) compared with undifferentiated ESCs; however, no significant differences were observed.

4 Discussion

If the chosen simulation approach in fact fulfills its requirements can be finally answered, when a corresponding experiment is performed under real microgravity conditions such as e.g. in the course of a spaceflight or parabolic flights.

The present results show that clinorotation affects the cytoskeleton, especially actin filaments, as well as the proliferation of murine embryonic stem cells and apoptosis from day 3 and 6 onwards. However, more investigations are required focusing on the cell cycle analysis from day 6 onwards as well as some studies focusing on the cytoskeleton, in combinations with methods e.g. Western Blot and qRT-PCR referring on protein and gene expressions related in forming the cytoskeleton. Moreover, there is one important aspect, which should be considered. The normal processing procedure of fixating embryonic stem cells has to be revised. Embryonic stem cells were exposed to simulated microgravity, but then the cells were centrifuged at e.g. 260 g for 5 min for e.g. changing the medium or for washing steps. It cannot be excluded that this strong hypergravity phase influenced the cells as well. However, the 1 g groups as well as the µ g groups were treated in the same way and, the significant differences with respect to cell cycle and changes of the cytoskeleton, clearly, indicate gravity-related effects. Furthermore, the staining procedure of embryonic stem cells and embryoid bodies has to be revised as well. In this study, the cells were blocked in BSA, which was not necessary. The blocking procedure is normally used for immunolabeling, a biochemical process that enables the detection of an antigen bound to a particular site within a cell or organ. In addition to that, some centrifugation steps and therefore the influence of the strong hypergravity phase may be prevented as well.

Some of the used methods in this study were applied for the first time. For further investigations the protocols have to be revised (e.g. the washing steps, cytoskeleton staining).

4.2 Hypergravity Experiments

In order to study the possible influence of hypergravity on the development of embryonic stem cells, several parameters were selected, which are involved in differentiation, pluripotency and cardiomyogenesis. In addition to that, the cell cycle and embryoid body morphology of ESCs were analyzed.

4.2.1 Hypergravity affects the Actin Cytoskeleton and Embryoid Body Morphology

Embryoid bodies derived from murine embryonic stem cells were exposed to hypergravity for specific time periods. EBs showed size variations in area and diameter at day 1 and 6; the diameters were significantly higher as compared to those under the 1 g control conditions. Interestingly, the 3 day exposed EBs did not show any significant changes in area and diameter. They were smaller in both parameters, which may be attributed to cell adaption to hypergravity conditions at a later time point, although there were changes observed after 24 hours. Wang et al. (2011) have reported that ESCs under simulated microgravity conditions (using a 3D clinostat) showed a decrease of adhesion rate, which normalized, when cells had adapted (approximately after 3 days). Possibly ESCs behave in the same way in a hypergravity environment. The changes in area and diameter of hypergravity-exposed ESCs were also reflected in morphological changes of EBs, which formed hyphae-like or dumbbell-shaped structures on day 1 and 3 as well as globular chains on day 6 as compared with samples from the control groups. These EB shapes were sensitive to any kind of treatments (e.g. the transfer into petri dishes resulted in isolated cells). Furthermore, in this study there were also qualitative differences in the cytoskeleton, precisely in the actin structure, observed. The exposure of ESCs to hypergravity resulted in a denser and tightly arranged actin framework as compared with the corresponding controls at 1 g on each time point, which indicate the capability of adaption to the environment. When the influence of the gravitational vector was intensified (1.8 g), cells obviously compensated the resulting force by forming, e.g. a more powerful cytoskeletal framework and thereby adapted to the hypergravity environment. It is questionable if the identified changes in EB morphology and

in the cytoskeleton are also reflected in their normal functions at the cellular level. It may be possible that some signaling pathways along the cytoskeletal framework are affected by the exposure to a hypergravity environment; further examinations should be performed for a better understanding of the phenomena observed, in combination with methods such as Western Blot and qRT-PCR referring on protein and gene expressions involved in forming the cytoskeleton. However, the results of the present study suggest that the EB shape definitely is influenced by hypergravity, which is also represented in the actin framework of EBs.

4.2.2 Effects of Hypergravity and Vibrations as Possible Side Effect on the Cell Cycle

In the course of the present study, the influence of hypergravity on the cell cycle distribution was investigated, finding a strong increase of cells in the SubG1-phase, but no significant changes were observed at any time point comparing the treatment with the control group. A strong increase of cell numbers in the SubG1-phase along with time in both gravity conditions has also been reported for cells, which were exposed to simulated microgravity (Wang et al., 2011), and is consistent with the results in this study (see chapter 3.1.2). Interestingly, the mean percentages of cells in SubG1-phase under the 1 *g* control conditions were as high as those which were exposed to hypergravity at each time point. Furthermore, it was expected that the mean percentages of cells in each cell cycle phase would be identical under both 1 *g* control conditions. i.e. the stationary samples in the incubator hosting either the centrifuge or the clinostat (see chapter 3.2.4). This was, however, not the case. In the 1 *g* controls of the clinostat experiments, more than 40 % of cells were arranged in the G1-phase, whereas only half of this percentage was arranged in the G1-phase in the 1 *g* control of the centrifuge experiments. A similar finding was the percentage of cells in the SubG1-phase between these two 1 *g* control conditions. 19 % of cells increased in the clinostat 1 *g* control and nearly 30 % of cells increased in the 1 *g* centrifuge control. It can be speculated that samples kept at the bottom of the centrifuge may experience vibrations due to the running of the centrifuge; it is assumed that such kind of vibrations do not occur in the clinostat, which has to be proven in the future. There were few studies performed

analyzing the impact of vibrations on e.g. chondrocytes, which suggested that vibrations were significantly detrimental to cartilage (Wehland et al., 2015; Ma et al., 2013). Consequently, vibrations might have an influence on embryonic stem cells. Furthermore, there were changes in EB morphology between the two control experiments in this study observed such as size and shape variances, which may be attributed to the vibrations of the running centrifuge as well (see chapter 3.2.1). This arises the question how to arrange appropriate 1 *g* controls, which also has been considered by Kamal et al. (2015).

4.2.3 Altered Gene Expression and Cardiomyogenesis in Hypergravity

Shinde et al. (2015) examined the influence of simulated microgravity on the expression of genes (Klf 4, Oct 4, CDH 1), which are able to induce a pluripotent and differentiated state in CGR8 embryonic stem cells, and they observed that these genes were not significantly affected. Moreover, they analyzed the expression of Myh 7, which is involved in cardiomyogenesis. When ESCs were exposed to simulated microgravity, the expression of Myh 7 was downregulated as compared with the 1 *g* control. Shinde et al. (2015) also found that EBs, when they were transferred to petri dishes at day 3 and subsequently cultured under similar conditions like the 1 *g* controls for additional 7 days, showed a reduced beating activity compared with the control group. Blaber et al. (2015) found a reduced expression in a number of cardiovascular differentiation markers, specifically in cardiomyocyte markers such as Myh 6 and Myh 7, which were downregulated in EBs differentiated in real µ *g*. Consequently, the expression of Klf 4, Oct 4, CDH 1 and Myh 6 as well as the expression of two more genes, namely cardiac Troponin and Nanog, was investigated in this study under hypergravity conditions. Unfortunately, the results of qRT-PCR were not evaluable because of the high fluctuations in the same conditions. The question of interest is whether the expression of Myh 6 and cardiac Troponin is upregulated or downregulated. Here, it may be possible that Myh 6 is upregulated due to the earlier contractions in EBs, which were found (averaged) at day 7.5, when ESCs were exposed for 3 and 6 days as compared with the findings in the corresponding control groups. This phenomenon also may

support the assumption that there are differences in the differentiation and pluripotency markers (CDH1, Oct 4, Klf 4, Nanog), which may cause a faster differentiation into cardiomyocytes under hypergravity conditions than under 1 *g*. Furthermore, there should be some experiments performed, which focus on the expression of cytoskeleton markers (e.g. tubulin and actin).

4.3 Conclusion and Outlook

Overall, the results of the present study suggest that clinorotation affects the actin system in embryonic stem cells and the cell cycle distribution. Moreover, the results suggest that also hypergravity has an impact on the differentiation potential, on cardiomyogenesis, and on EB morphology as well as on the actin framework of murine embryonic stem cells. Further investigations should be performed to study the effect of vibrations on the differentiation potential of ESCs. Furthermore, the commonly used and established procedures when experimenting with stem cells have to be considered. Examples are centrifugations of cells which have previously been exposed to simulated microgravity. However, as both – control and experiment samples – were processed after exposure in the same manner, a gravity-related effect can be discriminated. Nevertheless, a weak or no response might be obscured by centrifugation after clinorotation.

Mouse embryonic stem cells are able to differentiate into the three germ layers, recapitulating many aspects of the cell differentiation during early embryogenesis. Therefore they are a convenient *in vitro* model to analyze the impacts of simulated microgravity and hypergravity on the development. The cytoskeleton is known to be crucial for numerous cellular processes. In addition to this study, focusing on the actin framework during the exposure to simulated microgravity, changes in microtubules have to be considered, which may result in an altered or slowed down cell cycle distribution, particularly in mitosis and therefore in proliferation. These indications of the actin system could explain some of the mentioned dysmorphologies such as neural tube closure in the head (*Pleurodeles waltl*) or the different morphology of hatching *Xenopus* embryos occurring during their development in microgravity, as well as the lack of

development of mouse-embryos. Crawford-Young (2006) found that all cytoskeletal components were altered to some degree in microgravity which might have far reaching consequences if the cells are embryo cells. Another aspect, which has to be noticed, is that e.g. fish are able to produce live offspring in real microgravity (Crawford-Young, 2006) in contrast to rodents such as mice and rats. The underlying mechanisms of fertilization and embryogenesis under normal 1 *g* Earth gravity as well as under microgravity obviously depend on the given basic achievements of a biosystem to counter/use the gravitational force present or absent (Clément, 2005).

On the opposite, the results in the present study showed that hypergravity resulted in the formation of a denser and tightly arranged actin framework. Further studies should also focus on microtubules which may be more dynamic and in turn influence the cell cycle positively (e.g. faster proliferation rate). Differences in embryoid body morphology such as dumbbell-like structures may also indicate a high apoptosis rate, which may be attributed to the shape and size of EBs occurring during the development in hypergravity. On the other hand, the earlier contractions in EBs during the exposure to hypergravity may be a further indication for an extensive proliferation potential. It would be interesting to know, if the exposure of cells to hypergravity can counterbalance the effects on cells when they have previously been exposed to e.g. simulated or real microgravity, when the processing procedure is revised. In this case, providing hypergravity could be one of the main approaches, which can be used to antagonize effects due to microgravity (e.g. bone loss, skeletal muscle atrophy, cardiovascular problems, immune system dysregulation and alteration of sleep and circadian rhythms).

Taken together, the impact of gravity on embryonic stem cells differentiation is still not well understood. The availability of methods to alter the influence of gravity will help to identify underlying mechanism of embryogenesis.

5 Summary

Murine embryonic stem cells (ESCs) were exposed to simulated microgravity using the principle of a fast 2D clinostat and hypergravity (1.8 *g*) to investigate the effects of (altered) gravity on cell differentiation. In this context, gravity-induced changes in the cell cycle distribution, the gene expression, the cytoskeleton, the embryoid body morphology and the differentiation potential have been investigated. Changes in the gene expression and embryoid body morphology as well as reduced beating patterns (correlated with a lower expression of Myh 7) of ESCs after exposure demonstrated the impact of simulated microgravity. The analysis showed changes in the actin framework of the cytoskeleton on day 6 of clinorotation as compared with the corresponding 1 *g* controls; the actin framework was less pronounced under simulated microgravity conditions. Cell cycle analysis of clinorotated ESCs revealed significant changes in the G1-phase: the number of cells in the 1 *g* control group was significant higher as compared with the clinostat group. ESCs exposed to hypergravity revealed changes in the actin framework after 24 hours; the microfilaments were denser and tightly arranged than under 1 *g* conditions. Furthermore, hypergravity induced significant differences in the morphology of embryoid bodies regarding area and diameter and resulted in an increased size compared with the 1 *g* control, whereas the cell cycle seemed to be unaffected by hypergravity. Location of the 1 *g* control near to the centrifuge versus location of the 1 *g* control on the bottom of a clinostat revealed different numbers of cells in the SubG1-phase. This result indicates a potential device-specific side effect of vibration and in turn a combined effect of hypergravity and vibration on the running centrifuge. This has to be considered in further investigations.

As a result of the insufficient RNA quality and the fluctuating expression values of the investigated genes (Oct 4, Nanog, CDH 1, Myh 6, cardiac Troponin and Klf 4), there were no consistent results obtained in this study. However, increased beating activities in EBs may indicate changes in the expression of differentiation markers and in genes, which are involved in the process of cardiomyogenesis. The handling procedures of embryonic stem cells used in this study, have to be revised for further studies since standard laboratory procedures include e.g. centrifugation steps in order to concentrate cells, which might interfere with the gravity-related

experimental set-up. Overall, the results of this study suggest that embryonic stem cells are sensitive to altered gravity conditions and respond to gravity changes by e.g. forming a more/less powerful actin framework. Further investigations are necessary for understanding the effects of gravity and its effects on the actin cytoskeleton for the differentiation of ESCs and for understanding the development under altered gravity conditions.

Acknowledgment

First of all I would like to thank PD Dr. Ruth Hemmersbach since she gave me the possibility to perform my work in her working group at the German Aerospace Center (DLR) at Cologne and Prof. Dr. Johannes Bohrmann for taking over the role as the second-assessor at the University of Aachen. I would also like to thank Dr. Sonja Brungs (DLR) for valuable support, discussions and advices with my project as well as Vaibhav Shinde, Aviseka Acharya, Prof. Dr. Agapios Sachinidis and Prof. Dr. Jürgen Hescheler for the opportunity to perform a part of my experiments at the Institute for Neurophysiology at the University of Cologne. Furthermore, I would like to thank PD Dr. Christine Hellweg and Claudia Schmitz (DLR) for their help and advises in flow cytometry and cell cycle analysis as well as Prof. Dr. Christa Baumstark-Khan (DLR) for further analysis. I would further like to thank Kai Waßer, Dr. Jens Hauslage and Birgit Bromeis (DLR) for their support, help and advices in all laboratory work and for technical assistance. Prof. Dr. Ralf Anken (DLR) deserves special thanks for reading my thesis, discussions and valuable advices. Last but not least many thanks go to all members of the working group at DLR and to my family, since they support me continuously, no matter which questions I had.

References

Anken, R., Rahmann, H. (2002). Gravitational Zoology: How animals use and cope with gravity. Astrobiology: The Quest for the Conditions of Life, Springer-Verlag Berlin Heidelberg New York, Chapter 20, 316

Bishop, A. E., Buttery, L., Polak, J. M. (2002). Embryonic stem cells. Journal of Pathology, Vol 197, 424-429

Bishop, A. E., Rippon, H. J. (2004). Embryonic stem cells. Cell Proliferation, Vol 37, 23-34

Blaber, E., Finkelstein, H., Dvorochkin, N., Sato, K., Yousuf, R., Burns, B., Globus, R., Almeida, E. (2015). Microgravity reduces the differentiation and regenerative potential of embryonic stem cells. Stem Cells and Development, Vol 24, 1-40

Brungs, S., Egli, M., Wuest, S., Christianen, P., van Loon, J. (2015). Facilities for simulation of microgravity in the ESA ground-based facility programme. Microgravity Science and Technology, 1-10, DOI 10.1007/s12217-015-9462-9

Brungs, S. (2013). Influence of altered gravity on the oxidative burst in macrophages. Dissertation, University of Bonn

References

Buravkova, L. B., Romanov, Y. A., Konstantinova, N. A., Buravkov, S. V., Gershovich, Y. G., Grivennikov, I. A. (2008). Cultured stem cells are sensitive to gravity changes. Acta Astronautica, Vol 63, 603-608

Clément, G. (2005), Fundamentals of Space Medicine. Springer-Verlag Berlin Heidelberg New York, Chapter 1, 1

Crawford-Young, S. J. (2006). Effects of microgravity on cell cytoskeleton and embryogenesis. International Journal of Developmental Biology, Vol 50, 183-191

Evans, M. J., Kaufman, M. H. (1981). Establishment in culture of pluripotential cells from mouse embryos. Nature, Vol 292, 154-156

Frett, T., Petrat, G., van Loon, J., Hemmersbach, R., Anken, R. (2015). Hypergravity facilities in the ESA ground-based facility program – current research activities and future tasks. Microgravity Science and Technology, 1-10, DOI 10.1007/s12217-015-9462-9

Guignandon, A., Lafage-Proust, M., Usson, Y., Larohe, N. (2001). Cell cycling determines integrin-mediated adhesion in osteoblastic ROS 17/2.8 cells exposed to space-related conditions. The FASEB Journal, Vol 15, 2036-2038

Häder, P. D., Hemmersbach, R., Lebert, M. (2005). Gravity and the behavior of unicellular organisms. Cambridge University Press, Cambridge

References

Hescheler, J., Fleischmann, B. K., Lentini, S., Maltsev, V. A., Rohwedel, J., Wobus, A. M., Addicks, K. (1997). Embryonic stem cells: a model to study structural and functional properties in cardiomyogenesis. Cardiovascular Research, Vol 36, 149-162

Hemmersbach, R., von der Wiesche, M., Seibt, D. (2006). Ground-based experimental platforms in gravitational biology and human physiology Signal Transduction, Vol 6, 381-387

Herranz, R., Anken, R., Boonstra, J., Braun, M., Christianen, P., de Geerst, M., Hauslage, J., Hilbig, R., Hill, R., Labert, M., Medina, M., Vagt, N., Ullrich, O., van Loon, J., Hemmersbach, R. (2013). Ground-based facilities for simulation of microgravity: organism-specific recommendations for their use, and recommended terminology. Astrobiology, Vol 13, 1-17

Hu, L.F., Qian, A. R., Wang, Y., Di, S. M., Shang, P. (2012). Inhibitory effect of simulated microgravity on differentiating preosteoblasts. Advances in Space Research, Vol 51, 107-114

Istkovitz-Eldor, J., Schuldiner, M., Karsenti, D. (2000). Differentiation of human embryonic stem cells into embryoid bodies compromising the three embryonic germ layers. Molecular Medicine, Vol 6, 88-95

Jiao, F., Wang, J., Dong., Z.-L., Wu, M.-J., Zhao, T.-B., Li, D.-D., Wang, X. (2012). Human mesenchymal stem cells derived from limb bud can differentiate into all three embryonic germ layers lineages. Cellular Reprogramming, Vol 14, 324-333

References

Kamal, K., Hemmersbach, R., Medina, F., Herranz, R. (2015). Proper selection of 1 *g* controls in simulated microgravity research as illustrated with clinorotated plant cell suspension cultures. Life Sciences in Space, Vol 5, 47-52

Kawahara, Y., Manabe, M., Matsumoto M., Kajiume, T., Matsumuto, M., Yuge, L. (2009). LIF-free embryonic stem cell culture in simulated microgravity. PlosOne, Vol 4, 1-4

Kojima, Y., Sasaki, S., Kubota, Y., Ikeuchi, T., Hayashi, Y., Kohri, K. (2000). Effects of simulated microgravity on mammalian fertilization and preimplantation embryonic development *in vitro*. Fertility and Sterility, Vol 74, 1142-1147

Kurosawa, H. (2007). Methods for inducing embryoid body formation: *In vitro* differentiation system of embryonic stem cell. Journal of Bioscience and Bioengineering, Vol 103, 389-398

Livak, K. J., Schmittgen, T. D. (2001). Analysis of relative gene expression data using real-time quantitative PCR and the 2(-delta delta C(T)) method. Methods, Vol 25, 402-408

Li, J., Zhang, S., Chen, J., Du, T., Wang, Y. (2009). Modeled microgravity causes changes in the cytoskeleton and focal adhesions, and decreases in migration in malignant human MCF-7 cells. Protoplasma, Vol 238, 23-33

Ma, X., Wehland, M., Alechcheva, G., Hauslage, J., Waßer, K., Hemmersbach, R., Infanger, M., Bauer, J., Grimm, D. (2013). Interleukin-6 expression under gravitational stress due to vibration and hypergravity in follicular thyroid cancer cells. PlosOne, Vol 8, 1-12

References

McKinley, M., Dean O´Loughlin, V., Pennefather-O´Brian, E., Harris, R. (2015). Human Anatomy (4th Ed.). New York: McGraw Hill Education, 29

Nabavia, N., Khandanic, A., Camirandd, A., Harrison, R. (2011). Effects of microgravity on osteoclast bone resorption and osteoblast cytoskeletal organization and adhesion. Bone, Vol. 49, 965-974

Neff, A. W., Yokota, H., Chung, H. M., Wakahara, M., Malacinski, G. M. (1993). Early amphibian (Anuran) morphogenesis is sensitive to novel gravitational fields. Developmental Biology, Vol. 155, 270-274

Rösner, H., Wassermann, T., Möller, W., Hanke, W. (2006). Effects of altered gravity on the actin and microtubule cytoskeleton of human SH-SY5Y neuroblastoma cells. Protoplasma, Vol. 229, 225-234

Serova, L. V., Denisova, L. A., Apanasenko, Z. I., Meizerov, E. S. (1982). Reproductive function of the male rat after a flight on the Kosmos-1129 biosatellite. Kosmicheskaia Biologiia i Aviakosmicheskaia Meditsina, Vol 16, 62-65

Shinde, V., Brungs, S., Hescheler, J., Hemmersbach R., Sachinidis, A. (2015). Pipette-based method to study embryoid body formation derived from mouse and human pluripotent stem cells partially recapitulating early embryonic development under simulated microgravity conditions. Microgravity Science and Technology, 1-9, DOI 10.1007/s12217-015-9469-2

References

Smith, A. G., Heath, J. K., Donaldson, D. D., Wong, G. G., Moreau, J., Stahl, M., Rogers, D. (1988). Inhibition of pluripotential embryonic stem cell differentiation by purified polypeptides. Nature, Vol 336, 688-690

Thomson, J. A., Itskovitz-Eldor, J., Shapiro, S. S., Waknitz, M. A., Swiergiel, J.J., Marshall, V. S., Jones, J. M., (1998). Embryonic stem cell lines derived from human blastocysts. Science, Vol 282, 1145-1147

Uva, B., Masini, M., Sturla, M., Bruzzone, F, Giuliani, M. (2002). Microgravity-induced apoptosis in cultured glial cells. European Journal of Histochemistry, Vol 46, 209-214

Uva, B., Masini, M., Sturla, M., Pratoa, P., Passalacqua, M., Giuliani, M., Tagliafierro, G. Strollo, F. (2002). Clinorotation-induced weightlessness influences the cytoskeleton of glial cells in culture. Brain Research, Vol. 934, 132-139

Wang, Y., An, L., Jiang, Y., Hang, H. (2011). Effects of simulated microgravity on embryonic stem cells. PlosOne, Vol 6, 1-9

Wakayama, S., Kawahara, Y., Li, C., Yuge, L., Wakayama, T. (2009). Detrimental effects of microgravity on mouse preimplantation development *in vitro*. PlosOne, Vol 4, 1-10

References

White, J., Dalton, S. (2005). Cell cycle control of embryonic stem cells. Stem Cell Research, Vol 5, 131-138

Williams, R. L., Hilton, D. J., Pease, S., Willson, T. A., Stewart, C. L., Gearing, D. P., Wagner, E. F., (1988). Myeloid leukemia inhibitory factor maintains the developmental potential of embryonic stem cells. Nature, Vol 336, 684-687

Yabut, O., Bernstein, H. (2011). The promise of human embryonic stem cells in aging associated diseases. Aging , Vol 3, 494-508

Internet

Rowland, T. (2009). www.allthingsstemcell.com/glossary/#stemcells

Part, M. (2000). Introduction to flow cytometry: A learning guide. BD Biosciences; http://www.d.umn.edu/~biomed/flowcytometry/introflowcytometry.pdf

Appendix

List of Figures

Figure 1: The principle of clinorotation: cells in liquid media will sediment under normal gravity conditions (1 g) (left). Cells under real microgravity conditions will be randomly distributed and weightless (center). By the exposure on a 2D clinostat, cells will be rotated along one axis perpendicular to the direction of the gravity vector; microgravity is simulated due to the neutralization of sedimentation (right) (from Häder et al., 2005) *4*

Figure 2: Schematic representation of the isolation of ESCs: the blastocyst contains three components (the inner cell mass, the trophoblast and the blastocoel); ESCs are isolated from the inner cell mass of blastocysts and form all the tissues of the body; the three germ layers (mesoderm, ectoderm and endoderm) are formed during gastrulation (Yabut and Bernstein, 2011; edited by Wegener). *5*

Figure 3: Comparison of the schematic cell cycle structure of embryonic stem cells (ESCs) and embryoid bodies (EBs): M=Mitosis, S=Synthesis (S-phase), G1/G2=Gap phases (from White and Dalton, 2005; edited by Wegener). *8*

Figure 4: Embryo-derived pluripotent cells have an unusual cell cycle structure. Undifferentiated mESCs (left) and embryoid bodies (EBs) (right) derived from mESCs were stained with propidium iodide (PI) and analyzed by flow cytometry (from White and Dalton, 2005; edited by Wegener). *9*

Figure 5: Schematic representation of the experimental plan. *17*

Figure 6: A 2D-Pipette-Clinostat allows the exposure of ten 1 mL pipettes in parallel; 1 g controls are located at the bottom (arrow) (DLR, Cologne, Germany; designed by Dr. Jens Hauslage). *19*

Figure 7: Multi Sample Incubator Centrifuge: for incubation during hypergravity conditions of cell cultures different inserts have been constructed. Depending on the experimental demands, accelerations up to 40 g under controlled environmental conditions can be applied. 1 g controls are located at the side of the centrifuge (arrow) (DLR, Cologne, Germany). *22*

Figure 8: Example of flow cytometry analysis with FlowingSoftware 2.5.1 based on a pilot experiment: The first image (upper left) shows a dot plot of forward and side scatter, below is shown a typical cellular status with the majority of cells in the G0/G1 phase (left peak) and G2/M phase (rightmost peak). The area between these peaks indicates cells within the S-phase. The upper right image shows a dot plot of single cells, below, the statistics are shown. Further analysis can be done with Microsoft Excel. *26*

Figure 9: Actin cytoskeleton of cultured embryoid bodies after 1 day (A), 3 days (B) and 6 days (C): comparison of treatment (µ g) and control group (1 g); EBs were photographed with a confocal laser scanning fluorescence microscope; red: actin filaments (Phalloidin-Texas Red), blue: cell nuclei (DAPI), blue and red: merged. Scale bars: 100 µm. *32*

Figure 10: Comparison of cell cycle structure of undifferentiated mESCs (left) and embryoid bodies (EBs) (right) derived from mESCs, which were stained with propidium iodide (PI) and analyzed by flow cytometry. *34*

Appendix

Figure 11: Embryoid bodies derived from mESCs were stained with PI and analyzed by flow cytometry: comparison of cell cycle structure in CGR8 EBs, which were cultured in normal gravity (control group: 1 g) and simulated microgravity (treatment group: µ g) for different time periods. The data represent means of three experiments (n=3). 35

Figure 12: Morphological changes of cultured mESCs and EBs of CGR8 on days 1, 3 and 6 immediately after the exposure to hypergravity (1.8 g) in comparison to the control condition (1 g) in cell culture flasks. EBs were photographed with the stereomicroscope; scale bars: 1000 µm. 37

Figure 13: Morphological changes of cultured mESCs and EBs of CGR8 on days 1, 3 and 6 under 1 g conditions. EBs were photographed with the stereomicroscope; scale bars: 1 day: 100 µm; 3 days: 200 µm; 6 days: 300 µm. .. 38

Figure 14: Embryoid body reorganization: cells were exposed to hypergravity (1.8 g) for 1, 3 and 6 days and transferred into petri dishes until day 10 (central row). Within this timespan EBs reorganized their cell shape (bottom raw). EBs were photographed with the stereomicroscope. Scale bars: 1000 µm. 39

Figure 15: Morphological changes in area (A), diameter (B) and circularity(C) after incubation of ESCs under hypergravity or 1 g for different time periods in cell culture flasks. The data represent means ± standard errors of four independent experiments (n=4). 40

Figure 16: Cytoskeleton of cultured embryoid bodies after 1 day (A), 3 days (B) and 6 days (C): comparison of treatment (h g) and control group (1 g); EBs were photographed with a confocal laser scanning fluorescence microscope; red: actin filaments (Phalloidin-Texas Red), blue: cell nuclei (DAPI), blue and red: merged. Scale bars: 100 µm. 43

Figure 17: Embryoid bodies derived from mESCs were stained with PI and analyzed by flow cytometry: comparison of cell cycle structure in CGR8 EBs, which were cultured under normal gravity conditions (control group: 1 g) and hypergravity (treatment group: h g) for different time periods. The data represent means of four independent experiments (n=4). 45

Appendix

Statistical Analyses

Statistical analyses were performed with GraphPad Prism 5. Statistics were based on the Kolmogorov-Smirnov normality test. For cell cycle analysis and EB morphology (area, diameter and circularity) two-way Anova and Bonferroni post hoc tests were performed to evaluate the statistical significance. A P value of < 0.05 was considered statistically significant. In the following tables the statistics are shown: in the first column the time-span of an experimental/control run is provided, followed by two columns which represent the two gravity conditions (1 *g* vs µ *g*/ h *g* or 1 *g* vs 1 *g*). The column labeled *Difference* represents the difference of analyzed values obtained between the two conditions. The 95 % confidence interval (CI) is shown in the next column, which reflects a significance level of 0.05, the P value. The column which is labeled with *t* represents the post hoc test. The last column summarizes the statistical significance (ns= no significance, * = p < 0.05, ** = p < 0.01, *** = p < 0.001).

Embryoid Body Morphology

Two-way Anova and Bonferroni post hoc test

1 *g* circularity vs. h *g*_circularity							
Day of differ.	1 *g*_circ	hyp_circ	Difference	95% CI of diff.	t	P value	Summary
1	0.68	0.58	-0.09	-157.9 to 157.7	0	P > 0.05	ns
3	0.58	0.64	0.06	-157.7 to 157.9	0	P > 0.05	ns
6	0.7	0.58	-0.12	-157.9 to 157.7	0	P > 0.05	ns

1 *g*_diameter vs. h *g*_diameter							
Day of differ.	1 *g*_dia	h *g*_dia	Difference	95% CI of diff.	t	P value	Summary
1	274	414.2	140.2	-17.60 to 298.0	3	P < 0.05	*
3	254.6	341.2	86.55	-71.25 to 244.3	2	P > 0.05	ns
6	240.6	400.7	160.1	2.294 to 317.9	3	P<0.01	**

Appendix

1 *g*_area vs. h *g*_area							
Day of differ.	1 *g*_area	h *g*_area	Difference	95% CI of diff.	t	P value	Summary
1	40540	82040	41500	-7759 to 90750	3	P < 0.05	*
3	51550	62760	11210	-38040 to 60470	1	P > 0.05	ns
6	35120	96810	61680	12430 to 110900	4	P<0.001	***

Cell Cycle Analysis (µ *g*, h *g* vs. corresponding 1 *g* control)

Two-way Anova and Bonferroni post hoc test

1 *g*_G1 vs. µ *g*_G1							
Day	1 *g*_G1	µ *g*_G1	Difference	95% CI of diff.	t	P value	Summary
0	25.4	25.4	0	-11.35 to 11.35	0	P > 0.05	ns
1	29.75	31.57	1.823	-7.447 to 11.09	0.6512	P > 0.05	ns
3	31.43	29.77	-1.66	-10.93 to 7.611	0.5928	P > 0.05	ns
6	44.38	31.98	-12.4	-21.67 to -3.126	4.427	P<0.001	***

1 *g*_G2 vs. µ *g*_1G2							
Day	1 *g*_G2	*µ g*_1G2	Difference	95% CI of diff.	t	P value	Summary
0	42.03	42.03	0	-11.14 to 11.14	0	P > 0.05	ns
1	40.15	38.87	-1.287	-10.38 to 7.806	0.4685	P > 0.05	ns
3	34.64	35.63	0.9867	-8.106 to 10.08	0.3593	P > 0.05	ns
6	27.78	28.72	0.9367	-8.156 to 10.03	0.3411	P > 0.05	ns

Appendix

1 *g*_S-phase vs. µ *g*_S-phase							
Day	1 *g*_S	µ *g*_S	Difference	95% CI of diff.	t	P value	Summary
0	30.74	30.74	0	-9.759 to 9.759	0	P > 0.05	ns
1	29.03	26.57	-2.457	-10.42 to 5.511	1.021	P > 0.05	ns
3	23.57	24.85	1.28	-6.688 to 9.248	0.5319	P > 0.05	ns
6	14.39	18.77	4.383	-3.585 to 12.35	1.821	P > 0.05	ns

1 *g*_SubG1 vs. µ *g*_SubG1							
Day	1 *g*_SubG1	µ *g*_SubG1	Difference	95% CI of diff.	t	P value	Summary
0	1.33	1.33	0	-15.44 to 15.44	0	P > 0.05	ns
1	0.8767	2.373	1.497	-11.11 to 14.10	0.3931	P > 0.05	ns
3	10.2	9.277	-0.9267	-13.53 to 11.68	0.2434	P > 0.05	ns
6	13.3	19.15	5.853	-6.753 to 18.46	1.537	P > 0.05	ns

1 *g*_Polyploid vs. µ *g*_Polyploid							
Day	1 *g*_Pplyploid	µ *g*_Polyploid	Difference	95% CI of diff.	t	P value	Summary
0	0.51	0.51	0	-1.895 to 1.895	0	P > 0.05	ns
1	0.1967	0.62	0.4233	-1.124 to 1.971	0.9057	P > 0.05	ns
3	0.1567	0.4767	0.32	-1.228 to 1.868	0.6846	P > 0.05	ns
6	0.16	1.377	1.217	-0.3309 to 2.764	2.603	P > 0.05	ns

1 *g*_G1 vs. h *g*_G1							
Day	1 *g*_G1	h *g*_G1	Difference	95% CI of diff.	t	P value	Summary
0	22.58	22.58	0	-8.029 to 8.029	0	P > 0.05	ns
1	26.57	24.87	-1.7	-9.729 to 6.329	0.701	P > 0.05	ns
3	24.92	22.32	-2.595	-10.62 to 5.434	1.07	P > 0.05	ns
6	24.21	22.29	-1.918	-10.59 to 6.754	0.7324	P > 0.05	ns

Appendix

1 *g*_G2 vs. h *g*_G2							
Day	1 *g*_G2	h *g*_G2	Difference	95% CI of diff.	t	P value	Summary
0	38.56	38.56	0	-7.874 to 7.874	0	P > 0.05	ns
1	37.25	37.54	0.2975	-7.577 to 8.172	0.1251	P > 0.05	ns
3	27.34	27.18	-0.16	-8.034 to 7.714	0.06727	P > 0.05	ns
6	24.63	25.61	0.9883	-7.517 to 9.494	0.3847	P > 0.05	ns

1 *g*_S-phase vs. h *g*_S-phase							
Day	1 *g*_S	h *g*_S	Difference	95% CI of diff.	t	P value	Summary
0	37.03	37.03	0	-6.901 to 6.901	0	P > 0.05	ns
1	34.44	32.83	-1.607	-8.508 to 5.293	0.7713	P > 0.05	ns
3	25.35	28.84	3.488	-3.413 to 10.39	1.673	P > 0.05	ns
6	22.04	24.3	2.259	-5.194 to 9.713	1.004	P > 0.05	ns

1 *g*_SubG1 vs. h *g*_SubG1							
Day	1 *g*_SubG1	h *g*_SubG1	Difference	95% CI of diff.	t	P value	Summary
0	1.805	1.805	0	-10.92 to 10.92	0	P > 0.05	ns
1	1.58	4.56	2.98	-7.937 to 13.90	0.9037	P > 0.05	ns
3	22.36	21.36	-1.003	-11.92 to 9.915	0.304	P > 0.05	ns
6	29	27.63	-1.368	-13.16 to 10.42	0.3842	P > 0.05	ns

1 *g*_Polyploid vs. h *g*_Polyploid							
Day	1 *g*_Polyploid	h *g*_Polyploid	Difference	95% CI of diff.	t	P value	Summary
0	0.0325	0.0325	0	-1.340 to 1.340	0	P > 0.05	ns
1	0.1625	0.195	0.0325	-1.308 to 1.373	0.08029	P > 0.05	ns
3	0.03	0.305	0.275	-1.065 to 1.615	0.6794	P > 0.05	ns
6	0.14	0.1767	0.03667	-1.411 to 1.484	0.08386	P > 0.05	ns

Appendix

Cell Cycle Analysis (1 *g* (h *g*) vs. 1 *g* (µ *g*))

Two-way Anova and Bonferroni post hoc test

1 *g* (h *g*)_G1 vs. 1 *g* (µ *g*)_G1							
Day	1 *g* (hypergravity)	1 *g* (microgravity)	Difference	95% CI of diff.	t	P value	Summary
0	22.58	25.4	2.823	-7.010 to 12.66	0.9504	P > 0.05	ns
1	26.57	29.75	3.177	-5.495 to 11.85	1.213	P > 0.05	ns
3	24.92	31.43	6.516	-2.156 to 15.19	2.488	P > 0.05	ns
6	24.21	44.38	20.17	11.50 to 28.84	7.701	P<0.001	***

1 *g* (h *g*)_G2 vs. 1 *g* (µ *g*)_G2							
Day	1 *g* (hypergravity)	1 *g* (microgravity)	Difference	95% CI of diff.	t	P value	Summary
0	38.56	42.03	3.465	-6.179 to 13.11	1.19	P > 0.05	ns
1	37.25	40.15	2.908	-5.597 to 11.41	1.132	P > 0.05	ns
3	27.34	34.64	7.308	-1.197 to 15.81	2.845	P < 0.05	*
6	24.63	27.78	3.158	-5.347 to 11.66	1.229	P > 0.05	ns

1 *g* (h *g*)_S-phase vs. 1 *g* (µ *g*)_S-phase							
Day	1 *g* (hypergravity)	1 *g* (microgravity)	Difference	95% CI of diff.	t	P value	Summary
0	37.03	30.74	-6.285	-14.74 to 2.166	2.462	P > 0.05	ns
1	34.44	29.03	-5.411	-12.86 to 2.043	2.403	P > 0.05	ns
3	25.35	23.57	-1.783	-9.237 to 5.670	0.7922	P > 0.05	ns
6	22.04	14.39	-7.647	-15.10 to -0.1941	3.397	P<0.01	**

1 *g* (h *g*)_SubG1 vs. 1 *g* (µ *g*)_SubG1							
Day	1 *g* (hypergravity)	1 *g* (microgravity)	Difference	95% CI of diff.	t	P value	Summary
0	1.805	1.33	-0.475	-13.85 to 12.90	0.1176	P > 0.05	ns
1	1.58	2.373	0.7933	-11.00 to 12.59	0.2227	P > 0.05	ns
3	22.36	9.277	-13.09	-24.88 to -1.294	3.674	P<0.01	**
6	29	19.15	-9.845	-21.64 to 1.947	2.764	P < 0.05	*

Appendix

1 *g* (h *g*)_Polyploid vs. 1 *g* (μ *g*)_Polyploid							
Day	1 *g* (hypergravity)	1 *g* (microgravity)	Difference	95% CI of diff.	t	P value	Summary
0	0.0325	0.51	0.4775	-1.164 to 2.119	0.9631	P > 0.05	ns
1	0.1625	0.1967	0.03417	-1.413 to 1.482	0.07814	P > 0.05	ns
3	0.03	0.1567	0.1267	-1.321 to 1.574	0.2897	P > 0.05	ns
6	0.14	0.16	0.02	-1.428 to 1.468	0.04574	P > 0.05	ns